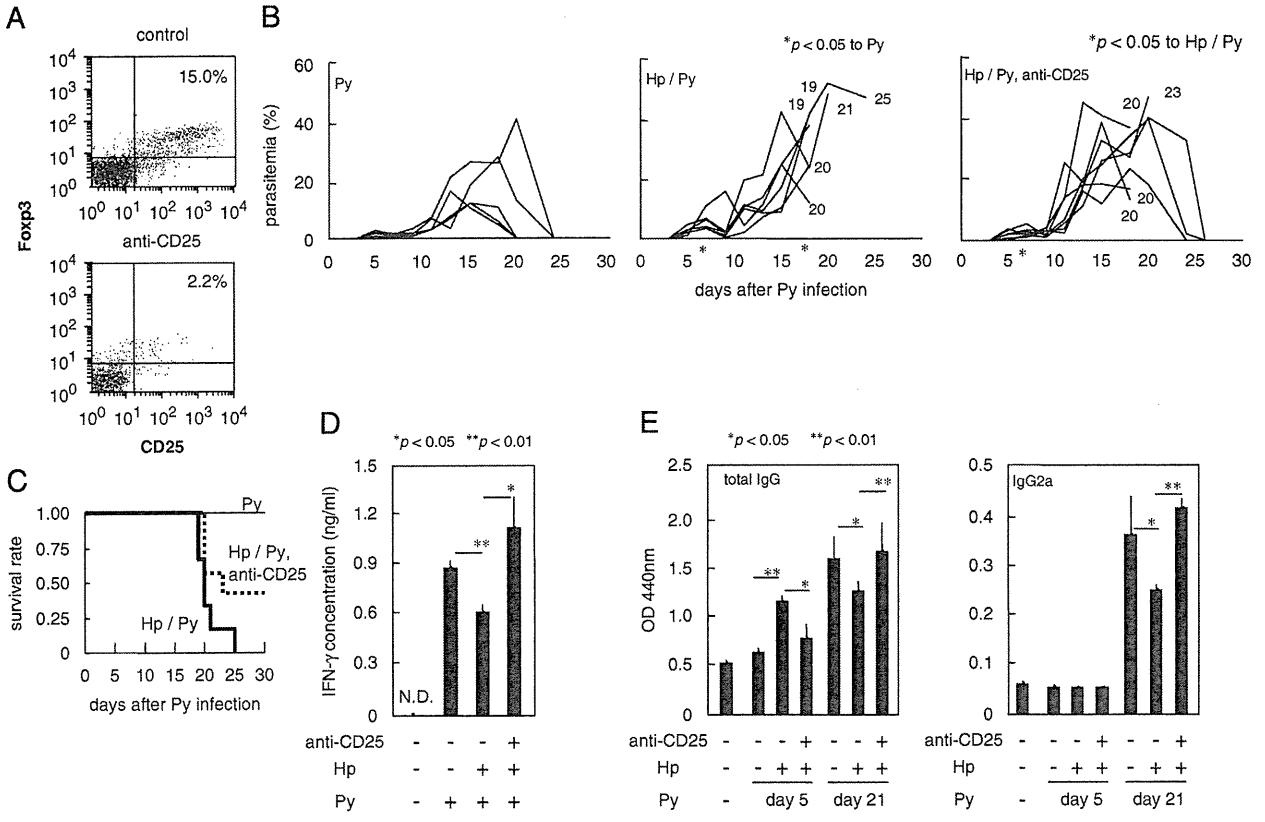

Figure 4. Effects of depletion of Treg in mice co-infected with Hp and Py. Spleen cells from mice depleted of Treg were analyzed as described in the legend for Fig. 3A. (A) The treatment depleted 85% of Treg in the spleen, as evaluated by flow cytometry on day 5 after Py infection. (B,C) Py infection in mice with or without depletion of Treg was monitored by the parasitemia (B) and survival (C) as described in the legend for Fig. 1. The infection experiments were repeated three times with similar results. (D, E) Immune responses and IFN-γ production in $CD4^+$ cells in response to pRBC (D) and serum levels of anti-Py IgG (E) were analyzed as described in the legend for Fig. 2. Data are presented as the means ±SE of three samples in a representative of 3–6 repeated experiments. Asterisks show significant differences at the indicated p values by Student's t-test.

with excretory/secretory (ES) Ag of Hp, an extract of adult Hp worms or living Hp worms in the presence of $CD11c^+$ DCs (Fig. 5). The cultured Treg were then analyzed for their suppressive activities. Treg cultured with medium alone still exhibited suppressive functions, although their effects were lower than those of freshly isolated Treg. However, none of the stimulatory conditions changed the suppressive abilities of the cultured Treg. The same tendency was observed when Treg were cultured without DC (data not shown) and when Treg from uninfected mice were stimulated with Hp preparations in combination with DC and pRBC, as well as without DC (data not shown). These results indicate that Hp worms residing in the intestine do not directly activate Treg.

Discussion

In the present study, we have demonstrated that a mouse intestinal nematode, Hp, was able to suppress anti-malaria protection *via* induction of Treg. Infection with malaria parasites is already known to activate Treg in humans and experimental models [3, 4], which allows rapid growth of malaria parasites. As previously reported [4], the non-lethal malaria parasite Py used in the present study does not strongly activate Treg and its low pathogenicity/virulence is closely linked to its failure to activate Treg. Therefore, it seems likely that activation of Treg in the presence of Hp converted the pathogenic behaviors of Py, as observed for a highly virulent *P. yoelii* strain [4]. Furthermore, the involvement of Treg activation for conversion to high virulence was clearly confirmed by the partial reversal of high parasitemia and mortality in mice depleted of Treg.

However, anti-CD25 treatment did not rescue all of the co-infected mice, partially because the depletion of Treg did not last longer than 2 wk. This finding may be supported by a previous observation that anti-CD25 treatment is insufficient because of a rapid expansion of Treg after infection with *P. yoelii* [27]. Interestingly, depletion of Treg recovered the suppression of presumably protective IgG responses at the late phase when Treg themselves reappeared comparably with the control Treg-sufficient mice. Therefore, besides activation of Treg, we cannot exclude various mechanisms supposed to cause the global immune suppression by intestinal helminths, regardless of the importance of Treg. For instance, the elevation of IgG1 observed at the early phase of infection suggests that Th2

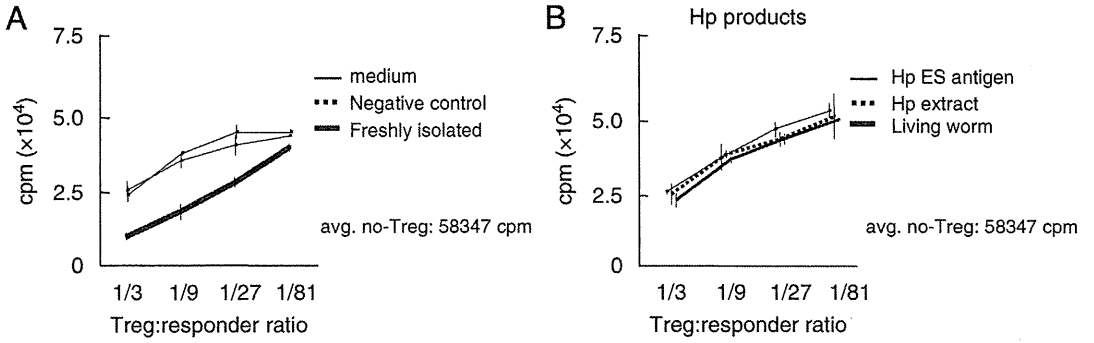

Figure 5. Stimulation of Treg with Hp products or living Hp worms *in vitro*. Splenic Treg isolated from mice at 5 days after Py infection were cultured with Hp products (100 μg/mL) or living Hp worms using a transwell system in the presence of DCs. Cultured Treg were used for suppressive analyses as described in the legend for Fig. 3C. Data are presented as the means ±SE of triplicate samples in a representative of 3–5 repeated experiments. There are no significant differences among the Treg conditioning treatments by Student's t-test.

responses in mice co-infected with Hp may prohibit the development of protective Th1 responses such as the production of IFN-γ.

Infections with helminths have also been reported to activate Treg [25, 28], and Hp suppresses allergic responses to innoxious Ag or protective immunity against pathogens in a Treg-dependent manner [29]. Su *et al.* [18] described the induction of regulatory cytokines, such as TGF-β and IL-10, during co-infection with Hp and *P. chabaudi*. We observed as well that transcription of TGF-β and IL-10 of Treg isolated from co-infected mice was slightly increased compared with those from non-infected animals or infected with either Py or Hp (data not shown). It would be interesting to evaluate the importance of these regulatory cytokines in *in vitro* suppressive function analysis, as done in Fig. 3C for instance.

The ES Ag of Hp were reported to be immunosuppressive toward T cells [30, 31]. However, we observed that infection with Hp alone did not activate Treg *in vivo* and that neither Hp products nor living worms directly activated Treg *in vitro*. Previous report suggested that Hp activates Treg *via* DC [32], but our *in vitro* results showed that Hp did not induce significant activation of Treg even in the co-culture with DC, suggesting less probability of the pathway between Hp *ex vivo* and strongly activated Treg, either dependently or independently of DC. One possibility may be that Hp infection takes longer than 2 wk to activate Treg by itself. Su *et al.* [18] described that mortality of co-infected mice increased if *P. chabaudi* infection was performed later than 2 wk after Hp infection. However, when we compared the effect of interval from preceding Hp to following Py infection on the induction of Treg between 2 and 6 wk (data not shown), Treg from both sets of co-infected mice showed similar and significant suppression compared with those from Py-infected mice, while Treg from Hp-infected mice did not show significant suppression. Taken together, our results suggest that Hp infection does not directly induce Treg activation, but probably conditions the host to stand by for Treg activation on exposure to incoming Ag /pathogens and/or enhances Treg activation by other stimulations such as Py.

Finally, our results demonstrate that co-infection with intestinal nematodes deteriorates the course of malaria, which is supposed to reflect the infectious state in malaria-endemic areas. Although we did not address whether treatment with anti-helminthic drugs improves malaria, chemotherapy against helminths would be included in global malaria control.

Materials and methods

Mice and parasites

Male 8- to 10-wk-old C57BL/6 mice were purchased from Kyudo (Tosu, Japan). All experiments using mice were conducted according to the guidelines for animal experimentation of Kyushu University.

Hp was kindly provided by Dr. J. F. Urban, Jr. (Beltsville Human Nutrition Research Center, US Department of Agriculture, Beltsville, MD, USA) and maintained by *in vivo* passages using male ICR mice. For infection, feces containing eggs were incubated on wet filter paper to allow the eggs to develop into infective larvae. Mice were infected orally with 200 infective larvae by gastric intubation. Infection was confirmed by Hp egg detection in feces before and after Py infection.

pRBC (2.5×10^4 cells/mouse) were commonly injected i.p., and the percent parasitemia (ratio of pRBC to total RBCs) was monitored by microscopic evaluation of thin blood films stained with Giemsa solution. For depletion of $CD25^+$ T cells *in vivo*, mice were injected i.p. with 100 μg of anti-CD25 Ab 1 day before and 1 day after Py infection. Each infection experiment was repeated three times with 5–7 mice *per* group.

Reagents

PE-anti-CD25 (PC61.5), allophycocyanin-anti-CD4 (GK1.5) and FITC-anti-Foxp3 (FJK-16s) staining kits, as well as FITC-anti-CD11c

(N418) Ab were obtained from eBioscience (San Diego, CA, USA). Anti-PE, anti-allophycocyanin and anti-FITC microbeads (Miltenyi Biotec GmBH, Bergisch Gladbach, Germany) were used for cell purification. Monoclonal rat anti-mouse CD25 (7D4) IgM purified from the ascites of hybridoma-injected athymic nude mice was used for *in vivo* treatments.

Preparation of parasites and their products

Worm products were prepared as described previously [30, 31] with modifications. Adult Hp worms were collected from the upper gastrointestinal tract of infected mice at 3–4 wk after larvae infection. The worms were washed three times with PBS containing ampicillin (150 μg/mL; Sigma, St. Louis, MO, USA) and streptomycin (50 μg/mL; Sigma), and approximately 500–1000 worms were incubated in 0.5 mL of ampicillin/streptomycin/PBS for 24–48 h at 37°C. The culture supernatant was collected by centrifugation at 10 000 × *g* for 10 min at 4°C and used as the Hp ES Ag. Worms were mechanically homogenized after or before incubation, and frozen and thawed 3–5 times. The supernatant was collected by centrifugation at 10 000 × *g* for 10 min at 4°C and used as the Hp extract. As a negative control, non-Hp-infected mouse intestinal contents were prepared in the same manner as for Hp ES Ag. All products were filtered through 0.45-μm pore filters, quantified by the BCA™ Protein Assay (Pierce, Rockford, IL, USA) and stored at –80°C until use. The products were pretreated with polymyxin B (50 μg/mL; Sigma) for 30 min before dilution with cell culture medium to a final concentration of 100 μg/mL, including 12.5 μg/mL polymyxin B. When required, living worms were freshly prepared by washing three times with PBS containing ampicillin and streptomycin and pretreated with polymyxin B for 30 min at room temperature. Hp products were prepared for each cellular experiment.

pRBC were isolated using a Percoll enrichment technique [33]. Briefly, blood from Py-infected mice was collected into heparinized PBS and passed through a cellulose column to remove leukocytes and platelets. After addition of the RBC solution to 63% v/v Percoll/PBS and centrifugation, pRBC were collected from the interphase. pRBC were freshly prepared for each cellular experiment. When required, isolated pRBC were frozen and thawed three times, and the supernatant was collected by centrifugation at 10 000 × *g* for 10 min at 4°C for use as a coating Ag in ELISA.

Cell purification

Cell purification was performed using a magnetic cell sorting system (Miltenyi Biotech GmBH) according to the manufacturer's instructions. Spleens of mice were reduced to single cell suspensions by hemolysis with 0.86% NH_4Cl. To purify $CD4^+CD25^-$ cells, the suspensions were incubated with FITC-anti-CD4 and PE-anti-CD25 Ab, followed by the addition of anti-PE microbeads and removal of $CD25^+$ cells. Anti-FITC microbeads were added to the flowthrough and $CD4^+CD25^-$ cells were obtained. DCs were purified using an FITC-anti-CD11c Ab. Treg were purified using a PE-anti-CD25 Ab, and 90% of them were confirmed to express CD4, CD25 and Foxp3 by flow cytometry. The purity of each cell subset usually exceeded 90%.

Cell culture

Purified T cells were cultured with pRBC in the presence of $CD11c^+$ cells in 200 μL of RPMI1640 supplemented with 100 IU/mL penicillin, 100 μg/mL streptomycin, 20 mM HEPES, 50 mM $NaHCO_3$, 2 mM L-glutamine, 100 μM 2-mercaptoethanol and 10% inactivated fetal bovine serum on round-bottomed 96-well plates. ConA was added as an assay control at a final concentration of 2.5 μg/mL. $CD11c^+$ cells were irradiated with 30 Gy before coculture with other cells. Typically, 1×10^5 T cells, $1–2 \times 10^5$ pRBC and 1×10^4 $CD11c^+$ cells were cocultured *per* well. Cultures were performed for 68–76 h at 37°C in air supplemented with 5% CO_2, including 10–16 h of coculture with ^{3}H-thymidine (1 μCi/well). Cells were harvested onto glass–fiber filter mats, dried and measured for their ^{3}H-thymidine uptake using a liquid scintillation counter. When required, the supernatant was collected before the addition of ^{3}H-thymidine and kept at –80°C until use. Each triplicate experiment was repeated 3–6 times.

Treg suppression assay

To analyze Treg functions, purified $CD4^+CD25^-$ cells (1×10^5 cells/well) from uninfected or infected mouse spleens stimulated with soluble ConA (2.5 μg/mL) and $CD11c^+$ cells (1×10^4 cells/well) from uninfected mouse spleens were cultured with a variety of freshly isolated or preconditioned Treg at various populations for 72 h and incubated with ^{3}H-thymidine (1 μCi/well) for the last 8–12 h. Radioactivity was measured using a liquid scintillation counter.

When required, purified Treg isolated from uninfected or Py-infected mouse spleens were preconditioned with $CD11c^+$ cells from uninfected mouse spleens under various conditions for 72 h. Conditioning with living Hp worms was performed using a transwell system (0.2-μm Anopore membrane; Nalge Nunc International, Rochester, NY, USA), in which the cells were in the lower chamber and 10 worms were in the upper chamber. Conditioned Treg were washed once, counted for living cells by Trypan blue staining and used for suppression assays as described above. Each triplicate experiment was repeated 3–5 times.

ELISA

The IFN-γ concentrations in the above-described cell culture supernatants were measured using a Mouse IFN-γ ELISA

Development Kit, DuoSet (R&D Systems, Minneapolis, MN, USA) according to the manufacturer's instructions. Each duplicate experiment was repeated three times. The anti-malaria Ab titers in the sera of mice were measured by ELISA by the OD at 440 nm using HRP-anti-mouse IgG(H+L), HRP-anti-mouse IgG1 and HRP-anti-mouse IgG2a Ab as previously described [34]. Sera were collected and kept at –80°C until analysis. Malaria Ag was prepared as described above and used as a coating Ag. Each triplicate experiment was repeated three times.

Flow cytometry

Splenocytes were prepared as single cell suspensions by hemolysis with 0.86% NH_4Cl. After staining of cell surface molecules or intracellular staining of Foxp3, the cells were evaluated using a FACSCalibur (BD, Franklin Lakes, NJ, USA) according to the manufacturer's instructions and the data were analyzed with the CellQuest Pro software (BD). Each infection experiment using 2–3 mice was repeated three times.

Statistical analysis

Student's *t*-test was used for statistical analyses. Values of $p<0.05$ were considered significant.

Acknowledgements: This study was supported by the Ministry of Education, Science, Sport and Culture of Japan (Grant 1890400, 19041056). The authors appreciate the special kindness of Dr. J. F. Urban Jr., Beltsville Human Nutrition Research Center, US Department of Agriculture, Beltsville, MD, USA, who provided the larvae of *Heligmosomoides polygyrus* used in this study.

Conflict of interest: The authors declare no financial or commercial conflict of interest.

References

1 Barry, A. E., Leliwa-Sytek, A., Tavul, L., Imrie, H., Migot-Nabias, F., Brown, S. M., McVean, G. A. V. *et al.*, Population genomics of the immune evasion (*var*) genes of *Plasmodium falciparum*. *PLoS Pathogens* 2007. **3**: e34.

2 Healer, J., Murphy, V., Hodder, A. N., Masciantonio, R., Gemmill, A. W., Anders, R. F., Cowman, A. F. *et al.*, Allelic polymorphisms in apical membrane antigen-1 are responsible for evasion of antibody-mediated inhibition in *Plasmodium falciparum*. *Mol. Microbiol.* 2004. **52**: 159–168.

3 Walther, M., Tongren, J. E., Andrews, L., Korbel, D., King, E., Fletcher, H., Andersen, R. F. *et al.*, Upregulation of TGF-beta, FOXP3, and $CD4^+CD25^+$ regulatory T cells correlates with more rapid parasite growth in human malaria infection. *Immunity* 2005. **23**: 287–296.

4 Hisaeda, H., Maekawa, Y., Iwakawa, D., Okada, H., Himeno, K., Kishihara, K., Tsukumo, S. and Yasutomo, K., Escape of malaria parasites from host immunity requires $CD4^+CD25^+$ regulatory T cells. *Nat. Med.* 2004. **10**: 29–30.

5 Xu, H., Wipasa, J., Yan, H., Zeng, M., Makobongo, M. O., Finkelman, F. D., Kelso, A. and Good, M. F., The mechanism and significance of deletion of parasite-specific $CD4^+$ T cells in malaria infection. *J. Exp. Med.* 2002. **195**: 881–892.

6 Urban, B. C., Ferguson, D. J. P., Pain, A., Willcox, N., Plebansk, M., Austyn, J. M. and Roberts, D. J., *Plasmodium falciparum*-infected erythrocytes modulate the maturation of dendritic cells. *Nature* 1999. **400**: 73–77.

7 March, K. and Snow, R. W., Malaria transmission and morbidity. *Parasitologia* 1999. **41**: 241–246.

8 Shankar, A. H., Nutritional modulation of malaria morbidity and mortality. *J. Infect. Dis.* 2000. **182**: S37–S53.

9 Barnes, K. I., Durrheim, D. N., Little, F., Jackson, A., Mehta, U., Allen, E., Dlamini, S. S. *et al.*, Effect of artemether-lumefantrine policy and improved vector control on malaria burden in KwaZulu-Natal, South Africa. *PLoS Med.* 2005. **2**: e330.

10 Abu-Raddad, L. J., Patnaik, P. and Kublin, J. G., Dual infection with HIV and malaria fuels the spread of both diseases in sub-Saharan Africa. *Science* 2006. **312**: 1603–1606.

11 World Health Organization, 2004. Malaria cases (per 100,000) by country, latest available data. Accessed on 28th January 2009.

12 World Health Organization, 2006. Soil-transmitted helminth (STH) infections are widely distributed in tropical and subtropical areas – 2006. Accessed on 28th January 2009.

13 Jenkins, S. J., Hewitson, J. P., Jenkins, G. R. and Mountford, A. P., Modulation of the host's immune response by schistosome larvae. *Parasite Immunol.* 2005. **27**: 385–393.

14 Hoerauf, A., Satoguina, J., Saeftel, M. and Specht, S., Immunomodulation by filarial nematodes. *Parasite Immunol.* 2005. **27**: 417–429.

15 Maizels, R. M. and Yazdanbakhsh, M., Immune regulation by helminth parasites: cellular and molecular mechanisms. *Nat. Rev. Immunol.* 2003. **3**: 733–744.

16 Nacher, M., Singhasivanon, P., Yimsamran, S., Manibunyong, W., Thanyavanich, N., Wuthisen, P. and Looareesuwan, S., Intestinal helminth infections are associated with increased incidence of *Plasmodium falciparum* malaria in Thailand. *J. Parasitol.* 2002. **88**: 55–58.

17 Nacher, M., Gay, F., Singhasivanon, P., Krudsood, S., Treeprasertsuk, S., Mazier, D., Vouldoukis I. and Looareesuwan, S., *Ascaris lumbricoides* infection is associated with protection from cerebral malaria. *Parasite Immunol.* 2000. **22**: 107–113.

18 Su, Z., Segura, M., Morgan, K., Loredo-Osti, J. C. and Stevenson, M. M., Impairment of protective immunity to blood-stage malaria by concurrent nematode infection. *Infect. Immun.* 2005. **73**: 3531–3539.

19 Noland, G. S., Urban, J. F., Jr. , Fried, B. and Kumar, N., Counter-regulatory anti-parasite cytokine responses during concurrent *Plasmodium yoelii* and intestinal helminth infections in mice. *Exp. Parasitol.* 2008. **119**: 272–278.

20 Tetsutani, K., Ishiwata, K., Torii, M., Hamano, S., Hisaeda, H. and Himeno, K., Concurrent infection with *Heligmosomoides polygyrus* modulates murine host response against *Plasmodium berghei* ANKA infection. *Am. J. Trop. Med. Hyg.* 2008. **79**: 819–822.

21 Gause, W. C., Urban, J. F., Jr., and Stadecker, M. J., The immune response to parasitic helminths: insights from murine models. *Trends Immunol.* 2003. **24**: 269–277.

22 Monroy, F. G. and Enriquez, F. J., *Heligmosomoides polygyrus*: a model for chronic gastrointestinal helminthiasis. *Parasitol. Today* 1992. **8**: 49–54.

23 Adachi, K., Tsutsui, H., Kashiwamura, S., Seki, E., Nakano, H., Takeuchi, O., Takeda, K. *et al.*, *Plasmodium berghei* infection in mice induces liver injury by an IL-12-and toll-like receptor/myeloid differentiation factor 88-dependent mechanism. *J. Immunol.* 2001. **167**: 5928–5934.

24 Shear, H. L., Srinivasan, R., Nolan, T. and Ng, C., Role of IFN-γ and nonlethal malaria in susceptible and resistant murine hosts. *J. Immunol.* 1989. **143**: 2038–2044.

25 Finney, C. A. M., Taylor, M. D., Wilson, M. S. and Maizels, R. M., Expansion and activation of $CD4^+CD25^+$ regulatory T cells in *Heligmosomoides polygyrus* infection. *Eur. J. Immunol.* 2007. **37**: 1874–1886.

26 Ohata, J., Miura, T., Johnson, T. A., Hori, S., Ziegler, S. F. and Kohsaka, H., Enhanced efficacy of regulatory T cell transfer against increasing resistance, by elevated Foxp3 expression induced in arthritic murine hosts. *Arthritis Rheum.* 2007. **56**: 2947–2956.

27 Couper, K. N., Blount, D. G., de Souza, J. B., Suffia, I., Belkaid, Y. and Riley, E. M., Incomplete depletion and rapid regeneration of $Foxp3^+$ regulatory T cells following anti-CD25 treatment in malaria-infected mice. *J. Immunol.* 2007. **178**: 4136–4146.

28 Watanabe, K., Mwinzi, P. N., Black, C. L., Muok, E. M., Karanja, D. M., Secor, W. E. and Colley, D. G., T regulatory cell levels decrease in people infected with *Schistosoma mansoni* on effective treatment. *Am. J. Trop. Med. Hyg.* 2007. **77**: 676–682.

29 Wilson, M. S., Taylor, M. D., Balic, A., Finney, C. A. M, Lamb, J. R. and Maizels, R. M., Suppression of allergic airway inflammation by helminth-induced regulatory T cells. *J. Exp. Med.* 2005. **202**: 1199–1212.

30 Telford, G., Wheeler, D. J., Appleby, P., Bowen, J. G. and Pritchard, D. I., *Heligmosomoides polygyrus* immunomodulatory factor (IMF), targets T-lymphocytes. *Parasite Immunol.* 1998. **20**: 601–611.

31 Rzepecka, J., Lucius, R., Doligalska, M., Beck, S., Rausch, S. and Hartmann, S., Screening for immunomodulatory proteins of the intestinal parasitic nematode *Heligmosomoides polygyrus*. *Parasite Immunol.* 2006. **28**: 463–472.

32 Segura, M., Su, Z., Piccirillo, C. and Stevenson, M. M., Impairment of dendritic cell function by excretory-secretory products: a potential mechanism for nematode-induced immunosuppression. *Eur. J. Immunol.* 2007. **37**: 1887-1904.

33 Tosta, C. E., Sedegah, M., Henderson, D. C. and Wedderburn, N., *Plasmodium yoelii* and *Plasmodium berghei*: isolation of infected erythrocytes from blood by colloidal silica gradient centrifugation. *Exp. Parasitol.* 1980. **50**: 7–15.

34 Matsuoka, Y., Malaria ELISA. In Tanabe, K., Waki, S., Kojima, S. and Kita, K. (Eds.), *Malariology Laboratory Manuals*. Kinokuniya, Tokyo 2000, pp. 123–126.

Abbreviations: **ES:** excretory/secretory · **Foxp3:** forkhead box p3 · **Hp:** *Heligmosomoides polygyrus* · **pRBC:** *Plasmodium yoelii*-parasitized erythrocyte · **Py:** *Plasmodium yoelii* 17XNL

Full correspondence: Dr. Kohhei Tetsutani, Department of Parasitology, Kyushu University Graduate School of Medical Science, 3-1-1 Maidashi, Higashi-ku, Fukuoka 812-0054, Japan
Fax: +81-92-642-6118
e-mail: tetztani@gmail.com

Received: 18/3/2009
Revised: 8/5/2009
Accepted: 24/6/2009

Vaccine 29 (2011) 2720–2726

Contents lists available at ScienceDirect

Vaccine

journal homepage: www.elsevier.com/locate/vaccine

Adenovirus-vectored Plasmodium vivax ookinete surface protein, Pvs25, as a potential transmission-blocking vaccine

Takeshi Miyata[a], Tetsuya Harakuni[a], Hideki Sugawa[a,b], Jetsumon Sattabongkot[c], Aki Kato[d], Mayumi Tachibana[e], Motomi Torii[e], Takafumi Tsuboi[d], Takeshi Arakawa[a,f,]

[a] Molecular Microbiology Group, Department of Tropical Infectious Diseases, COMB, Tropical Biosphere Research Center, University of the Ryukyus, 1 Senbaru, Nishihara, Okinawa 903-0213, Japan
[b] AMBiS Corporation, 2013 Ozato, Nanjyo, Okinawa 901-1202, Japan
[c] Department of Entomology, Armed Forces Research Institute of Medical Sciences, Bangkok 10400, Thailand
[d] Cell-Free Science and Technology Research Center, Ehime University, 3 Bunkyo-cho, Matsuyama, Ehime 790-8577, Japan
[e] Department of Molecular Parasitology, Ehime University, Graduate School of Medicine, Shitsukawa, Toon, Ehime 791-0295, Japan
[f] Division of Host Defense and Vaccinology, Graduate School of Medicine, University of the Ryukyus, 207 Uehara, Nishihara, Okinawa 903-0215, Japan

ARTICLE INFO

Article history:
Received 10 September 2010
Received in revised form
29 December 2010
Accepted 21 January 2011
Available online 11 February 2011

Keywords:
Malaria transmission-blocking vaccine
Human adenovirus

ABSTRACT

Adjuvants or delivery vehicles are essential components to expedite malaria vaccine development. In this study, replication-defective human adenovirus serotype 5 (rAd) was genetically engineered to express the Plasmodium vivax ookinete surface protein (OSP), Pvs25 (AdPvs25). BALB/c mice immunized with the AdPvs25 through various routes including intramuscular, subcutaneous and intranasal routes were analyzed for induction of antigen-specific transmission-blocking immunity. Parenteral but not mucosal immunization induced high serum immunoglobulin G (IgG) responses specific to P. vivax ookinetes isolated from P. vivax volunteer patients from Thailand. The membrane feeding assay revealed that antisera conferred a transmission blockade of up to 99% reduction in the average oocyst numbers per mosquito, while immunization with a rAd expressing Pfs25 from Plasmodium falciparum, a homolog of Pvs25, conferred only a background level of blockade, suggesting that a species-specific transmission-blocking immunity was induced. Vaccine efficacy of AdPvs25 was slightly higher than to a recombinant Pvs25 protein mixed with aluminum hydroxide, but less efficacious than the protein emulsified with incomplete Freund's adjuvant. This study, the first preclinical evaluation of adenovirus-vectored malaria OSPs, implicates a potential inclusion of malaria transmission-blocking vaccine antigens in viral vector systems.

1. Introduction

Malaria is one of the most serious infectious diseases with high mortality and morbidity in large areas of tropical regions of the world. There were estimated 189–327 million cases and 881,000 malaria deaths in 2006 [1]. The majority of victims of malaria are children in sub-Saharan Africa. Implementation of various control measures including drug therapy and insecticide-treated bednets have made a substantial contribution to reduction of malaria cases over the past decades; however, these control measures are not sufficient partly due to the emergence of parasites resistant to antimalarial drugs and mosquito strains resistant to insecticides, and hence new prevention tools need to be developed for local elimination and the ultimate eradication of the disease [2–4]. The development of effective and affordable vaccines is therefore believed to benefit global public health by closing the gap left by the current malaria intervention measures [5].

Several promising vaccine candidates have been intensively investigated [6,7], such as those targeting sporozoite [8], hepatic and erythrocytic stages [9], which are designed to prevent infection and to reduce disease severity. On the other hand, transmission-blocking vaccines (TBVs) that target the sexual stage, in which the parasite undergoes sporogonic development in anopheline mosquitoes, prevent parasite transmission in the mosquito [10–12]. TBVs induce antibodies that react with the ookinete surface proteins (OSPs) of malaria parasites within the mosquito midgut, and as such they do not directly protect vaccinated individuals from infection. They could however contribute to elimination of the disease by lowering the parasite transmission

Corresponding author at: Molecular Microbiology Group, Department of Tropical Infectious Diseases, COMB, Tropical Biosphere Research Center, University of the Ryukyus, 1 Senbaru, Nishihara, Okinawa 903-0213, Japan.
Tel.: +81 98 895 8974; fax: +81 98 895 8974.
E-mail address: tarakawa@comb.u-ryukyu.ac.jp (T. Arakawa).

0264-410X/$ – see front matter © 2011 Elsevier Ltd. All rights reserved.
doi:10.1016/j.vaccine.2011.01.083

frequency below the threshold at which the parasite can maintain its life cycle [2,13,14]. Additionally, TBVs, if combined with vaccines targeting other infection stages, could prevent transmission of escape mutants that emerge during infection. Therefore, TBVs might function as a "safety net" for pre-erythrocytic and erythrocytic vaccines, as well as other non-vaccine interventions.

Plasmodium falciparum causes the highest mortality rates among the four Plasmodium species known to infect humans; however Plasmodium vivax, the second most prevalent malaria species, causes 80–300 million clinical cases every year [15], has the highest morbidity and is a major cause of recurrent malaria. Its clinical manifestations range from asymptomatic to severe diseases that in some cases lead to death. Additionally, an increase in the number of severe cases of P. vivax infection casts doubts regarding what was thought to be its relatively benign nature [16]. This species is therefore an important target of malaria control efforts [5,13–15,17]. Furthermore, because global malaria eradication is the ultimate goal, the value of developing vaccines against P. vivax can no longer be underestimated [5,13–15,17].

The majority of malaria vaccine candidate antigens currently under preclinical and clinical evaluation are recombinant in origin [6,7], and therefore they are only marginally immunogenic by themselves. This has been demonstrated to be true for the two P. vivax candidate vaccine antigens recently tested in clinical trials, the circumsporozoite protein (CSP) [13,18] and Pvs25 OSP [13,19,20]. Therefore, appropriate adjuvant formulations or employment of delivery systems seem to be extremely important in inducing an optimal antiparasite immune response.

Replication-defective human adenovirus has been intensively evaluated for the delivery of foreign genes in gene therapy and for vaccine development against infectious diseases including malaria [21–23]. The ability to induce both cell-mediated and humoral immunities as well as a long-lasting memory T cell response are generally considered advantages of the viral vector systems in vaccine development against malaria [21,23,24]. Those immunities are important to confer solid protection against infection [25]. Attenuated adenovirus has been used for US military recruits to prevent respiratory infection [23,26], therefore safety issues may not be a serious concern for this viral vector system. P. falciparum antigens at the pre-erythrocytic stage such as CSP and liver-stage antigen-1 (LSA1), and antigens at the erythrocytic stage such as apical membrane antigen-1 (AMA1) and merozoite surface protein-1 (MSP1) are being tested in clinical trials as adenovirus-vectored antigens [7,23].

Since TBVs require efficient antibody-inducing capacity [10–12,27–30], we therefore hypothesized that the adenovirus vector system is beneficial for this purpose. In this study we evaluated potential application of a replication-defective human adenovirus serotype 5 to induce transmission-blocking immunity against P. vivax malaria. The vaccine efficacy of the induced mouse antisera was evaluated by a membrane-feeding assay using field strains of parasites obtained from P. vivax volunteer patients in Thailand.

2. Materials and methods

2.1. Immunization with a recombinant adenovirus expressing Pvs25

AdPvs25 is a replication-defective human adenovirus serotype 5, expressing the Pvs25 gene under the regulation of the cytomegalovirus enhancer and promoter [31]. Genetic engineering of AdPvs25 was conducted based on a COS-TPC method, according to the manufacturer's instructions (TAKARA Bio, Otsu, Japan). Recombinant Pvs25 (rPvs25) protein expressed and purified from the methylotrophic yeast Pichia pastoris [27] was used to comparatively evaluate immunogenicity of AdPvs25.

Eight-week-old female BALB/c mice were purchased from Japan SLC (Shizuoka, Japan), and housed in a special pathogen-free environment in our research institute. Mice were immunized four times at weeks 0, 3, 5 and 7 via subcutaneous (s.c.; 100 μl at a single injection site), intramuscular (i.m.; 50 μl at two injection sites), intranasal (i.n.; 15 μl into each nostril), or intragastric (i.g.; 200 μl) route with 5.1×10^9 plaque forming units/ml of AdPvs25, or three times at weeks 0, 2 and 4 via the s.c. route with 30 μg of the rPvs25 protein alone, or with incomplete Freund's adjuvant (IFA; Difco Laboratories, Detroit, MI, USA) or aluminum hydroxide (Alum; Pierce, Rockford, IL, USA) as controls.

All animal experimental protocols used in this study were approved by the Institutional Animal Care and Use Committee of the University of the Ryukyus, and the experiments were conducted according to the Ethical Guidelines for Animal Experiments of the University of the Ryukyus.

2.2. ELISA for antibody titer determination

Mouse antisera were collected 1–2 weeks after the last immunization (week 8 or 6 for AdPvs25 or rPvs25 protein, respectively), and Pvs25-specific serum IgG was analyzed by ELISA as described previously [27–30]. Briefly, the ELISA plates (Sumilon; Sumitomo Bakelite Co., Ltd., Tokyo, Japan) were coated with 5 μg/ml of rPvs25 in bicarbonate buffer overnight at 4 C and blocked with 1% (w/v) bovine serum albumin (BSA) in phosphate buffered saline (PBS) for 2 h at 37 C. Two-fold serial dilutions of the antisera, commencing with an initial 50-fold dilution with 0.5% (w/v) BSA in PBS, were applied to wells (2 h, 37 C). Anti-mouse IgG conjugated to alkaline phosphatase (1/4000; Sigma–Aldrich, St. Louis, MO, USA) was added to the wells and incubated for 2 h at 37 C, before its substrate p-nitrophenylphosphate (Bio-Rad Laboratories, Inc., Redmond, WA, USA) was applied for 20 min at 37 C and the absorbance at 415 nm (OD_{415}) was read on a microplate reader (Bio-Rad). The plates were washed twice with PBS containing 0.05% Tween-20 (PBS-T) and once with PBS between each incubation step. The antibody titer was defined as the serum dilution that gave an OD_{415} value equal to 0.1, or as the serum dilution where a one magnitude higher dilution gave an OD_{415} value less than 0.1.

2.3. Mosquito membrane feeding assay

The membrane feeding assay was conducted as described previously [27–29]. Briefly, peripheral blood was collected, with written informed consent, from P. vivax volunteer patients who came to a malaria clinic in the Mae Sod district in the Tak province of northwestern Thailand. Plasma was removed from the collected blood. Single species infection with P. vivax was confirmed by Giemsa stain prior to the assay. The vaccine-induced mouse antisera were mixed with an equal volume of heat-inactivated human AB serum obtained from malaria-naïve volunteers. Then, the mouse antisera and the human AB serum mixture was added to the parasitized blood cells obtained from the patients (1:1 v/v ratio), and incubated for 15 min at room temperature. The mixture was applied to a membrane feeding apparatus kept at 37 C to feed Anopheles dirus A mosquitoes (Bangkok colony, Armed Forces Research Institute of Medical Sciences) for 30 min. Fully engorged mosquitoes were maintained for a week in an insectary kept at 26 C. For each test sample, 20 mosquitoes were analyzed to count the number of oocysts that had developed in the midgut.

Human subject research conducted in this study was reviewed and approved by the Ethics Committee of the Thai Ministry of Public Health and the Institutional Review Board of the Walter Reed Army Institute of Research.

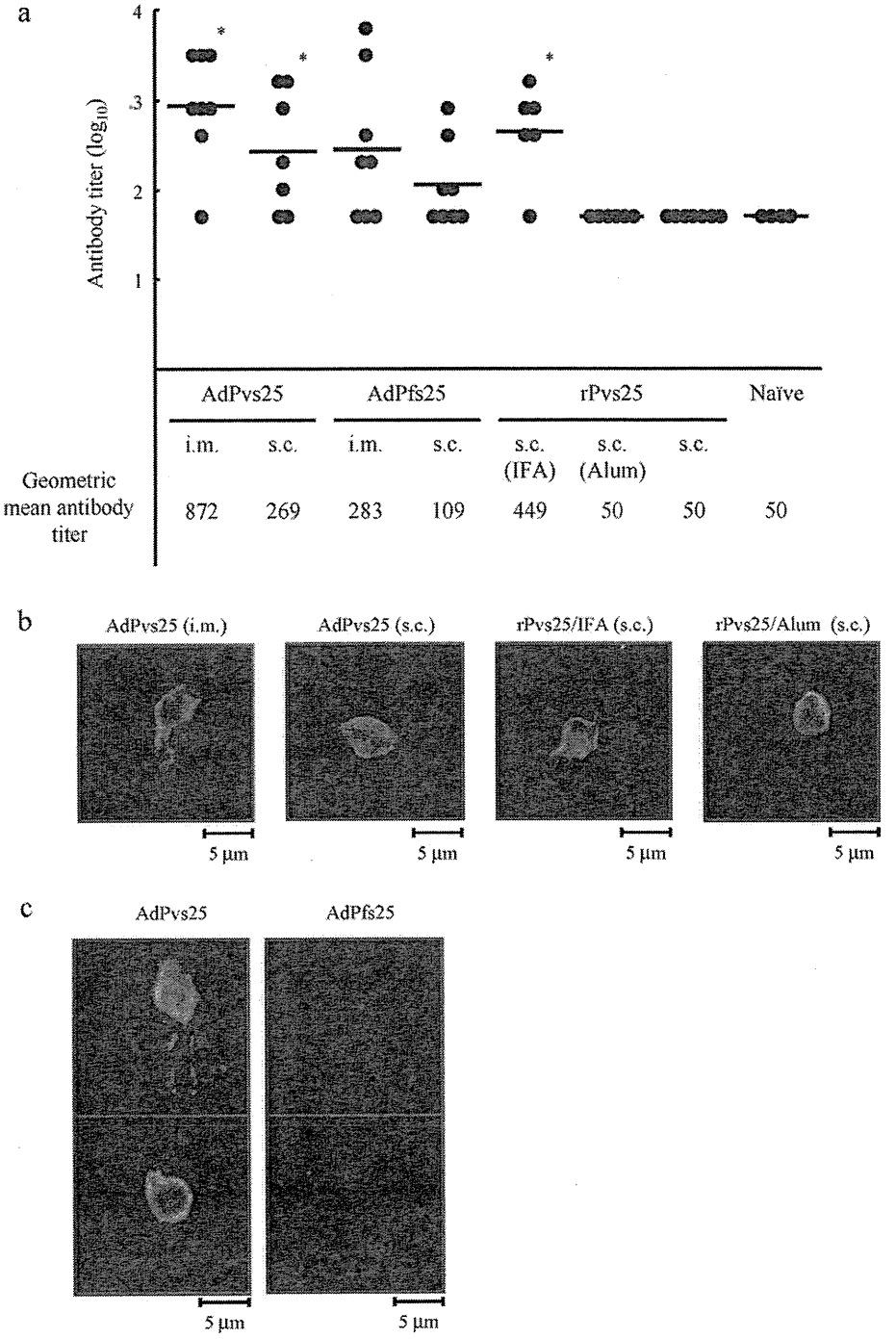

Fig. 1. Immunogenicity of AdPvs25 in mice. (a) Eight-week-old female BALB/c mice were immunized four times at weeks 0, 3, 5 and 7 via subcutaneous (s.c.) or intramuscular (i.m.) route with 5.1×10^8 plaque forming units of the AdPvs25, or three times at weeks 0, 2 and 4 via the s.c. route with 30 μg of recombinant Pvs25 (rPvs25) protein alone, or with incomplete Freund's adjuvant (IFA) or aluminum hydroxide (Alum), as controls. Serum samples were collected at week 8 or 6 for the adenovirus-vectored or the recombinant protein immunization, respectively, and evaluated for Pvs25-specific IgG titers. Serum from naïve mice was used as a negative control for the ELISA. Antibody titers were defined as the serum dilution that resulted in an OD_{415} of 0.1, or as the serum dilution where a one magnitude higher dilution gave an OD_{415} value less than 0.1. * indicates a significant difference to non-immune serum by the Wilcoxon–Mann–Whitney test ($P < 0.05$). (b) Ookinete-specific reactivity of the induced antisera as analyzed by immunofluorescence. The antisera derived from i.m. or s.c. immunization with the AdPvs25, or s.c. immunization with the rPvs25 protein emulsified with IFA or the rPvs25 protein mixed with Alum specifically recognized native Pvs25 protein expressed on the surface of P. vivax zygote/immature ookinetes. (c) The antisera derived from i.m. immunization with the AdPvs25 or the AdPfs25 were reacted to P. vivax zygote/immature ookinetes, indicating the specificity of the AdPvs25 antisera.

2.4. Detection of native Pvs25 using mouse antisera

Peripheral blood of P. vivax-infected volunteer patients was collected as described above. The gametocytemic blood was used to grow zygotes and ookinetes in vitro [32], then samples were spotted onto slides and fixed with acetone as described previously [27–30]. The slides were then blocked with 5% nonfat milk in PBS, and incubated with the mouse antiserum derived from immunization with

the AdPvs25, AdPfs25, or the rPvs25 protein emulsified with IFA, or the rPvs25 protein mixed with Alum, after diluting the antisera 100-fold with 5% nonfat milk in PBS. The samples were washed with ice-cold PBS and incubated with Alexa488-conjugated anti-mouse antibody (Invitrogen, Carlsbad, CA, USA). After washing with ice-cold PBS, slides were viewed by confocal scanning laser microscopy (LSM5 PASCAL; Carl Zeiss MicroImaging, Thornwood, NY, USA).

2.5. Statistical analysis

Statistical analyses were conducted by the Wilcoxon–Mann–Whitney test or the Kruskal–Wallis test using JMP software version 8.0 (SAS Institute, Inc., Cary, NC, USA).

3. Results and discussion

There is an increasing demand for the development of effective recombinant vaccine platform technologies to enhance vaccine efficacy by the innovation of new adjuvants or delivery systems [33]. This would seem to be particularly true for OSPs, because they are low-molecular-weight proteins that are by themselves not sufficiently immunogenic.

In this study, we engineered replication-defective human adenovirus serotype 5 for expression of a P. vivax OSP, Pvs25, to test its efficacy to induce transmission-blocking immunity. We immunized BALB/c mice through various routes including i.m., s.c., i.n. and i.g., and the Pvs25-specific serum IgG response was measured (Fig. 1a and Table 1). Parenteral (i.m. and s.c.) but not mucosal (i.n. and i.g.) immunization (Supplementary data Fig. 1) with the AdPvs25 induced robust IgG responses comparable in titers to those induced by the rPvs25 protein administered s.c. with IFA. Immunization by the i.m. route with the AdPvs25 tended to induce higher IgG response than s.c. immunization, and at least three booster injections seemed to be necessary to induce the maximal level of response (Supplementary data Fig. 1). AdPvs25-induced antisera could efficiently recognize the P. vivax ookinete surface as determined by the immunofluorescence assay (Fig. 1b). Although, rPvs25 protein immunization with aluminum hydroxide induced only a background level of IgG response as compared with the unimmunized naïve control serum (Fig. 1a), the induced antiserum could recognize the parasite surface as efficiently as the AdPvs25 or the rPvs25/IFA induced antiserum (Fig. 1b).

AdPfs25 immunization, particularly for the i.m. route, induced relatively high IgG response to the rPvs25 protein as determined by ELISA (Fig. 1a and Supplementary data Fig. 2), implicating that the induced antisera are somewhat cross-reactive at least at the recombinant protein level; however, the differences in IgG titers between AdPfs25 and the unimmunized naïve control groups did not reach statistically significant levels. Further, AdPfs25 antisera failed to react to the P. vivax ookinete (Fig. 1c), indicating the specificity of the AdPvs25 antisera.

Next, we evaluated the TBV efficacy of the induced mouse antisera against field isolates of P. vivax parasites in infected blood samples from volunteer patients in Thailand by the membrane feeding assay as described previously [28,29]. The same experiments were performed three times using blood samples from three different P. vivax (Pv)-infected volunteer donors (Pv-infected blood donors 1–3; Fig. 2a–c and Table 1). The average number of oocysts per mosquito fed on parasitized blood mixed with the antisera induced by parenteral immunization (i.m. or s.c.) with the AdPvs25 was reduced by 82–99% as compared with the unimmunized naïve control serum when parasite burden was low (Fig. 2a and b and Table 1). Although, the rPvs25/Alum induced no detectable Pvs25-specific serum IgG response (Fig. 1a and Table 1), its TBV efficacy (92–97% blockade; Fig. 2a and b and Table 1) was com-

Table 1
Summary of immunization experiments outlining antibody titers and transmission-blocking effects.

Immunization group	Immunization route	Adjuvant	Geometric mean antibody titer	TBV effect (Pv-infected blood donor 1)		TBV effect (Pv-infected blood donor 2)		TBV effect (Pv-infected blood donor 3)	
				Average oocyst number per mosquito (median oocyst number)	% Reduction in average oocyst number per mosquito (oocyst-free mosquitoes per 20 mosquitoes)	Average oocyst number per mosquito (median oocyst number)	% Reduction in average oocyst number per mosquito (oocyst-free mosquitoes per 20 mosquitoes)	Average oocyst number per mosquito (median oocyst number)	% Reduction in average oocyst number per mosquito (oocyst-free mosquitoes per 20 mosquitoes)
AdPvs25	i.m.	–	872§	1.5* (1.0)	82.3 (9)	0.1* (0)	98.6 (19)	10.0* (3.0)	71.4 (7)
	s.c.	–	269§	1.0* (0)	87.8 (11)	1.3* (0)	82.4 (13)	25.0 (14.5)	28.5 (1)
AdPfs25	i.m.	–	283	10.0 (7.0)	0 (4)	5.5 (5.0)	25.7 (3)	85.3 (71.5)	0 (0)
	s.c.	–	109	16.6 (18.0)	0 (1)	7.9 (6.0)	0 (1)	207.3 (206.0)	0 (0)
rPvs25	s.c.	IFA	449§	0* (0)	100 (20)	0* (0)	100 (20)	0* (0)	100 (20)
	s.c.	Alum	50	0.7* (0)	91.5 (13)	0.2* (0)	97.3 (17)	31.2 (24.5)	10.9 (1)
	s.c.	–	50	7.0 (6.0)	14.6 (1)	1.4* (0.5)	81.1 (10)	53.5 (34.0)	0 (1)
Naïve		–	50	8.2 (7.5)	0 (3)	7.4 (4.5)	0 (5)	35.0 (14.5)	0 (0)

i.m.: intramuscular; s.c.: subcutaneous; IFA: incomplete Freund's adjuvant; Alum: aluminum hydroxide; TBV: transmission-blocking vaccine; Pv: Plasmodium vivax.
* $P < 0.001$ vs. naïve.
§ $P < 0.005$ vs. naïve.
% Reduction is calculated as the reduction in the average oocyst number for each immunization group compared to the average oocyst number for the unimmunized naïve control group.

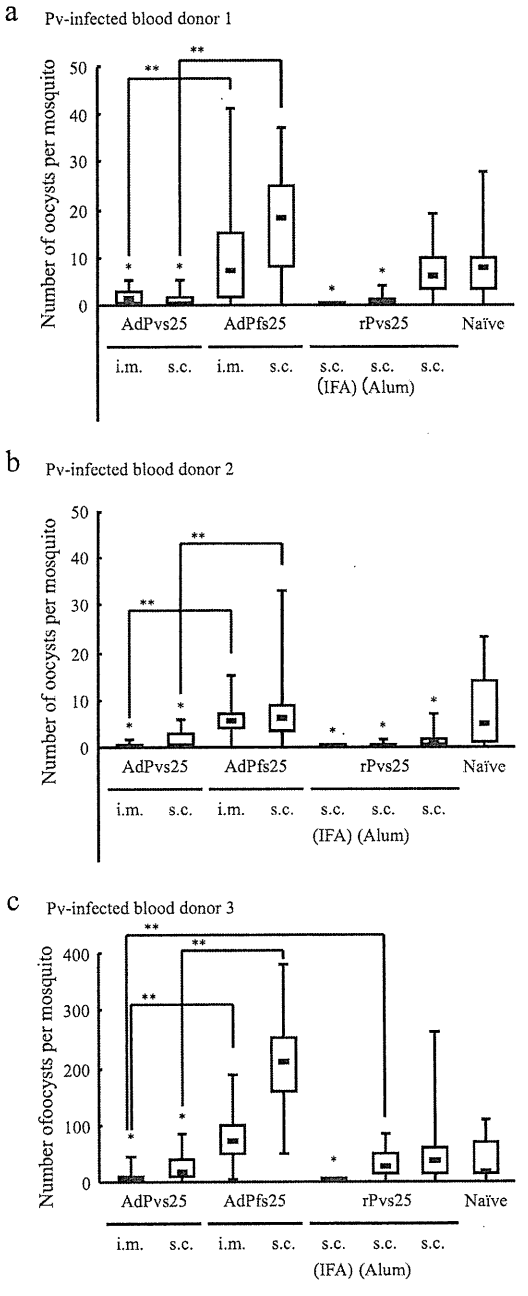

Fig. 2. Transmission-blocking effects induced by antisera (1/2 dilution) derived from mice immunized with the AdPvs25, the AdPfs25, or the rPvs25 protein were evaluated. The data were expressed as the median values of oocyst number per mosquito (black bar within the box) with 25% and 75% quartiles (box) and ranges (error bars). Three independent experiments were performed, using three blood samples from Pv-infected blood donors 1–3. * $P<0.001$ vs. naïve mice by the Wilcoxon–Mann–Whitney test; ** $P<0.001$ between the indicated two groups by the Wilcoxon–Mann–Whitney test.

parable to those attained by the AdPvs25. We do not know why the rPvs25/Alum immunization conferred substantial TBV efficacy without inducing antibody response detectable in ELISA (Fig. 1a); however, when the level of parasite burden increased as seen in the case for donor 3, the AdPvs25 appeared to become significantly more efficacious than the rPvs25/Alum, particularly for the i.m. immunization regimen (Fig. 2c and Table 1). These results suggest that adenovirus-vectored Pvs25 has potentially higher vaccine efficacy than the Alum-adjuvanted rPvs25 protein.

The rPvs25/IFA immunization consistently conferred a complete blockade regardless of the level of parasite burden; however, the local reactogenicity was considerably higher than Alum-adjuvanted or adenovirus-vectored immunization regimen.

Intraperitoneal or intravenous immunization with the AdPvs25 induced a robust serum IgG response, although its TBV effect was not assessed in this study. In contrast, despite the fact that adenoviruses mainly affect the respiratory system, the AdPvs25 administered by the i.n. route failed to induce a specific serum IgG response as determined by the ELISA (Supplementary Fig. 1). This might be due to the fact that only a low virus dose was able to be administered. However, the rPvs25 protein administered i.n. with a minute amount of cholera toxin (CT) adjuvant consistently induced a strong IgG response in mice, and as such its level of efficacy was very similar to that attained by the i.m. administered AdPvs25 immunization regimen (data not shown). Thus, it seems that adenovirus-vectored i.n. immunization is much less effective than the recombinant protein antigen administered through the same route with a potent mucosal adjuvant like CT. Administration through the i.g. route was also tested in this study, but failed to induce any antibody response, probably because the gastrointestinal environment is too destructive for the virus to effectively transduce the foreign gene. The intravaginal route was found to be another ineffective route to induce an antibody response by adenovirus immunization, and as such no specific serum IgG was observed. The reason for this failure might be the same as those for i.n. immunization.

In this study we concomitantly engineered a replication-defective adenovirus expressing Pfs25, an ortholog gene of Pvs25. Its immunization induced low but detectable cross-reactive serum IgG to the rPvs25 protein, although it did not reach a level of statistical significance as compared with the naïve control serum (Fig. 1a). However, the membrane feeding assay confirmed that no TBV effect was induced against P. vivax species (Fig. 2), suggesting that induction of interspecies cross-blocking immunity cannot be expected. However, a mixed administration of the two adenovirus vectors each expressing Pfs25 and Pvs25, or engineering of a single virus vector that co-expresses both P25 genes should be technically feasible, implicating that multi-species TBVs could be constructed. To address this possibility, we conducted a preliminary immunization experiment in which a mixture of the two adenoviruses, AdPfs25 and AdPvs25, were administered through various routes, and assessed immunogenicity towards both proteins. The results implicated that the existence of multiple viral vectors did not have a negative impact on the induction of specific IgG responses against the individual protein (data not shown).

Heterologous prime–boost regimens employing different viral vectors, different administration routes, or different vaccine formulations such as those using plasmid DNA or recombinant proteins, is thought to be a promising approach to enhance vaccine efficacy of malaria antigens [23,34–38]. To determine whether the prime–boost regimen is also applicable to OSP-based TBVs, we tested a DNA prime-adenovirus vector boost (one DNA injection and three consecutive adenovirus injections). The results implicated however that DNA immunization does not adequately replace adenovirus vector immunization, because the level of antibody remained lower than the adenovirus vector only immunization regimen (data not shown). Similarly, a combination of different immunization routes was evaluated and from our results, we concluded that replacement of parenteral with mucosal immunization induced a lower immune response (data not shown). Taken together, these results implicate that DNA or mucosal immunization, which was by itself found not to be sufficiently immunogenic, when combined with the parenteral adenovirus vector immunization, ablated to varying degrees the

overall vaccine efficacy. However, we were unable to make a final conclusive statement, at this preliminary stage of evaluation, regarding the suitability of a prime–boost regimen and whether or not it could be applied for TBVs. This is because there are other various possible combinations that need to be tested, such as an adenovirus prime–vaccinia virus boost regimen, which is known to be one of the most effective combinations [36,38].

Since OSP-based TBVs do not directly protect vaccinated individuals from infection, it should not be used as a "standalone" malaria vaccine. Researchers are beginning to realize that a single antigen, a single stage, or even a single species malaria vaccine developmental strategy can no longer be considered as a practical or realistic strategy, as was previously believed [5], and therefore a combination of heterologous immunization regimens, including the prime–boost method, need to be pursued more vigorously for future malaria vaccine development. In this sense, it is very feasible and should be technically possible to combine adenovirus-vectored TBVs with other virus vectored vaccines, such as vaccinia virus, or with viral vectors targeting the pre-erythrocytic or erythrocytic stages of single or multiple malaria species, or even in combination with vaccines targeting other infectious diseases.

Of course, there is still much scope for optimizing adenovirus-vectored OSP-based TBVs. For example, adenovirus serotype 5 used in the present study may need to be changed to other serotypes for future clinical application in malaria endemic areas in Africa, because a large proportion of African population has high serotype 5 antibody [37]. However, the present study should at least support the notion that malaria OSP antigens can be included in adenovirus-vectored or possibly other viral vectored immunization regimens, and that they are able to induce comparable levels of humoral immunity compared with those induced by the recombinant proteins combined with the Alum adjuvant.

Acknowledgments

We thank the staff of the Armed Forces Research Institute of Medical Sciences in Bangkok, Thailand, for their technical assistance. This work was supported by grants from the Program of Founding Research Centers for Emerging and Reemerging Infectious Diseases from The Ministry of Education, Culture, Sports, Science and Technology, Japan (MEXT); Grants-in-Aid for Scientific Research (19406009 and 20590425) and Scientific Research on Priority Areas (21022034) from MEXT; a grant from the Okinawa Industry Promotion Public Corporation; and the Cooperative Research Grant of the Institute of Tropical Medicine, Nagasaki University.

Appendix A. Supplementary data

Supplementary data associated with this article can be found, in the online version, at doi:10.1016/j.vaccine.2011.01.083.

References

[1] WHO. World Health Report. 2008.
[2] Greenwood BM, Fidock DA, Kyle DE, Kappe SH, Alonso PL, Collins FH, et al. Malaria: progress, perils, and prospects for eradication. J Clin Invest 2008;118(4 (April)):1266–76.
[3] Targett GA, Greenwood BM. Malaria vaccines and their potential role in the elimination of malaria. Malar J 2008;7(Suppl. 1):S10.
[4] Genton B. Malaria vaccines: a toy for travelers or a tool for eradication? Expert Rev Vaccines 2008;7(5 (July)):597–611.
[5] PATH malaria vaccine initiative: about the malaria vaccine roadmap. Available from: http://www.malariavaccineorg/malvac-roadmap.php.
[6] Sharma S, Pathak S. Malaria vaccine: a current perspective. J Vector Borne Dis 2008;45(1 (March)):1–20.
[7] WHO. Malaria vaccine rainbow tables. Available from: http://www.who.int/vaccine_research/links/Rainbow/en/index.html.
[8] Ballou WR. The development of the RTS,S malaria vaccine candidate: challenges and lessons. Parasite Immunol 2009;31(9 (September)):492–500.
[9] Richards JS, Beeson JG. The future for blood-stage vaccines against malaria. Immunol Cell Biol 2009;87(5 (July)):377–90.
[10] Tsuboi T, Tachibana M, Kaneko O, Torii M. Transmission-blocking vaccine of vivax malaria. Parasitol Int 2003;52(1 (March)):1–11.
[11] Kaslow DC. Transmission-blocking vaccines: uses and current status of development. Int J Parasitol 1997;27(2 (February)):183–9.
[12] Carter R. Transmission blocking malaria vaccines. Vaccine 2001;19(17–19 (March)):2309–14.
[13] Arevalo-Herrera M, Chitnis C, Herrera S. Current status of Plasmodium vivax vaccine. Hum Vaccin 2010;6(1 (January)).
[14] Birkett AJ. PATH malaria vaccine initiative (MVI): perspectives on the status of malaria vaccine development. Hum vaccin 2010;6(1 (January)):139–45.
[15] Sina B. Focus on Plasmodium vivax. Trends Parasitol 2002;18(7 (July)):287–9.
[16] Kochar DK, Das A, Kochar SK, Saxena V, Sirohi P, Garg S, et al. Severe Plasmodium vivax malaria: a report on serial cases from Bikaner in northwestern India. Am J Trop Med Hyg 2009;80(2 (February)):194–8.
[17] Bill and Melinda Foundation. Global Health Program. Available from: http://www.gatesfoundation.org/global-health/Documents/malaria-strategy.pdf.
[18] Herrington DA, Nardin EH, Losonsky G, Bathurst IC, Barr PJ, Hollingdale MR, et al. Safety and immunogenicity of a recombinant sporozoite malaria vaccine against Plasmodium vivax. Am J Trop Med Hyg 1991;45(6 (December)):695–701.
[19] Malkin EM, Durbin AP, Diemert DJ, Sattabongkot J, Wu Y, Miura K, et al. Phase 1 vaccine trial of Pvs25H: a transmission blocking vaccine for Plasmodium vivax malaria. Vaccine 2005;23(24 (May)):3131–8.
[20] Wu Y, Ellis RD, Shaffer D, Fontes E, Malkin EM, Mahanty S, et al. Phase 1 trial of malaria transmission blocking vaccine candidates Pfs25 and Pvs25 formulated with montanide ISA 51. PLoS ONE 2008;3(7):e2636.
[21] Li S, Locke E, Bruder J, Clarke D, Doolan DL, Havenga MJ, et al. Viral vectors for malaria vaccine development. Vaccine 2007;25(14 (March)):2567–74.
[22] Draper SJ, Heeney JL. Viruses as vaccine vectors for infectious diseases and cancer. Nat Rev Microbiol 2010;8(1 (January)):62–73.
[23] Limbach KJ, Richie TL. Viral vectors in malaria vaccine development. Parasite Immunol 2009;31(9 (September)):501–19.
[24] Reyes-Sandoval A, Harty JT, Todryk SM. Viral vector vaccines make memory T cells against malaria. Immunology 2007;121(2 (June)):158–65.
[25] Beeson JG, Osier FH, Engwerda CR. Recent insights into humoral and cellular immune responses against malaria. Trends Parasitol 2008;24(12 (December)):578–84.
[26] Russell KL, Hawksworth AW, Ryan MA, Strickler J, Irvine M, Hansen CJ, et al. Vaccine-preventable adenoviral respiratory illness in US military recruits, 1999–2004. Vaccine 2006;24(15 (April)):2835–42.
[27] Miyata T, Harakuni T, Tsuboi T, Sattabongkot J, Kohama H, Tachibana M, et al. Plasmodium vivax ookinete surface protein, Pvs25, linked to cholera toxin B subunit induces potent transmission-blocking immunity by intranasal as well as subcutaneous immunization. Infect Immun 2010.
[28] Arakawa T, Komesu A, Otsuki H, Sattabongkot J, Udomsangpetch R, Matsumoto Y, et al. Nasal immunization with a malaria transmission-blocking vaccine candidate, Pfs25, induces complete protective immunity in mice against field isolates of Plasmodium falciparum. Infect Immun 2005;73(11 (November)):7375–80.
[29] Arakawa T, Tsuboi T, Kishimoto A, Sattabongkot J, Suwanabun N, Rungruang T, et al. Serum antibodies induced by intranasal immunization of mice with Plasmodium vivax Pvs25 co-administered with cholera toxin completely block parasite transmission to mosquitoes. Vaccine 2003;21(23 (July)):3143–8.
[30] Arakawa T, Tachibana M, Miyata T, Harakuni T, Kohama H, Matsumoto Y, et al. Malaria ookinete surface protein-based vaccination via the intranasal route completely blocks parasite transmission in both passive and active vaccination regimens in a rodent model of malaria infection. Infect Immun 2009;77(12 (December)):5496–500.
[31] Kass-Eisler A, Li K, Leinwand LA. Prospects for gene therapy with direct injection of polynucleotides. Ann NY Acad Sci 1995;772(November):232–40.
[32] Suwanabun N, Sattabongkot J, Tsuboi T, Torii M, Maneechai N, Rachapaew N, et al. Development of a method for the in vitro production of Plasmodium vivax ookinetes. J Parasitol 2001;87(4 (August)):928–30.
[33] O'Hagan DT, Valiante NM. Recent advances in the discovery and delivery of vaccine adjuvants. Nat Rev Drug Discov 2003;2(9 (September)):727–35.
[34] Kongkasuriyachai D, Bartels-Andrews L, Stowers A, Collins WE, Sullivan J, Sattabongkot J, et al. Potent immunogenicity of DNA vaccines encoding Plasmodium vivax transmission-blocking vaccine candidates Pvs25 and Pvs28-evaluation of homologous and heterologous antigen-delivery prime–boost strategy. Vaccine 2004;22(23–24 (August)):3205–13.
[35] Coban C, Philipp MT, Purcell JE, Keister DB, Okulate M, Martin DS, et al. Induction of Plasmodium falciparum transmission-blocking antibodies in nonhuman primates by a combination of DNA and protein immunizations. Infect Immun 2004;72(1 (January)):253–9.
[36] Reyes-Sandoval A, Berthoud T, Alder N, Siani L, Gilbert SC, Nicosia A, et al. Prime–boost immunization with adenoviral and modified vaccinia virus Ankara vectors enhances the durability and polyfunctionality of pro-

tective malaria CD8+ T-cell responses. Infect Immun 2010;78(1 (January)): 145–53.
[37] Hill AV, Reyes-Sandoval A, O'Hara G, Ewer K, Lawrie A, Goodman A, et al. Prime–boost vectored malaria vaccines: progress and prospects. Hum vaccin 2010;6(1 (January)).
[38] Bruna-Romero O, Gonzalez-Aseguinolaza G, Hafalla JC, Tsuji M, Nussenzweig RS. Complete, long-lasting protection against malaria of mice primed and boosted with two distinct viral vectors expressing the same plasmodial antigen. Proc Natl Acad Sci USA 2001;98(20 (September)):11491–6.

Parasitology International 60 (2011) 132–138

Contents lists available at ScienceDirect

Parasitology International

journal homepage: www.elsevier.com/locate/parint

Plasmodial ortholog of *Toxoplasma gondii* rhoptry neck protein 3 is localized to the rhoptry body

Daisuke Ito [a], Eun-Taek Han [b], Satoru Takeo [a], Amporn Thongkukiatkul [c], Hitoshi Otsuki [d], Motomi Torii [e], Takafumi Tsuboi [a,f,*]

[a] *Cell-Free Science and Technology Research Center, Ehime University, Matsuyama, Ehime 790-8577, Japan*
[b] *Department of Parasitology, Kangwon National University College of Medicine, Chuncheon, Republic of Korea*
[c] *Department of Biology, Faculty of Science, Burapha University, Chonburi 20131, Thailand*
[d] *Division of Medical Zoology, Faculty of Medicine, Tottori University, Yonago, Tottori 683-8503, Japan*
[e] *Department of Molecular Parasitology, Ehime University Graduate School of Medicine, Shitsukawa, Toon, Ehime 791-0295, Japan*
[f] *Venture Business Laboratory, Ehime University, Matsuyama, Ehime 790-8577, Japan*

ARTICLE INFO

Article history:
Received 23 November 2010
Received in revised form 24 December 2010
Accepted 7 January 2011
Available online 13 January 2011

Keywords:
Cell-free expression
Erythrocyte invasion
Merozoite
Plasmodium falciparum
Rhoptry

ABSTRACT

The proteins in apical organelles of *Plasmodium falciparum* merozoite play an important role in invasion into erythrocytes. Several rhoptry neck (RON) proteins have been identified in rhoptry proteome of the closely-related apicomplexan parasite, *Toxoplasma gondii*. Recently, three of *P. falciparum* proteins orthologous to *TgRON* proteins, *Pf*RON2, 4 and 5, were found to be located in the rhoptry neck and interact with the micronemal protein apical membrane antigen 1 (*Pf*AMA1) to form a moving junction complex that helps the invasion of merozoite into erythrocyte. However, the other *P. falciparum* RON proteins have yet to be characterized. Here, we determined that "PFL2505c" (hereafter referred to as *pfron3*) is the ortholog of the *tgron3* in *P. falciparum* and characterized its protein expression profile, subcellular localization, and complex formation. Protein expression analysis revealed that *Pf*RON3 was expressed primarily in late schizont stage parasites. Immunofluorescence microscopy (IFA) showed that *Pf*RON3 localizes in the apical region of *P. falciparum* merozoites. Results from immunoelectron microscopy, along with IFA, clarified that *Pf*RON3 localizes in the rhoptry body and not in the rhoptry neck. Even after erythrocyte invasion, *Pf*RON3 was still detectable at the parasite ring stage in the parasitophorous vacuole. Moreover, co-immunoprecipitation studies indicated that *Pf*RON3 interacts with *Pf*RON2 and *Pf*RON4, but not with *Pf*AMA1. These results suggest that *Pf*RON3 partakes in the novel *Pf*RON complex formation (*Pf*RON2, 3, and 4), but not in the moving junction complex (*Pf*RON2, 4, 5, and *Pf*AMA1). The novel *Pf*RON complex, as well as the moving junction complex, might play a fundamental role in erythrocyte invasion by merozoite stage parasites.

1. Introduction

Malaria is caused by the replication of protozoan parasites of the genus *Plasmodium* in circulating host erythrocytes [1]. The invasion process of merozoite stage parasite into erythrocyte requires the discharge of contents of apical secretory organelles (micronemes and rhoptries) to form an irreversible contact, called a tight junction, between the merozoite and the erythrocyte membrane. This tight junction migrates from the anterior to posterior poles of the merozoite. According to this moving junction, the host membrane invaginates the merozoites to eventually form a parasitophorous vacuole [2,3]. The moving junction is one of the most distinctive features of apicomplexan invasion into host cells, and was first observed in *Plasmodium* species [4]. Studies in apicomplexan parasite *Toxoplasma gondii* identified a total of four proteins from distinct apical secretory organelles to form a moving junction complex; micronemal protein apical membrane antigen 1 (AMA1) and three rhoptry neck (RON) proteins, RON2, RON4, and RON5 [5,6]. Recently, this RON–AMA1 complex (*Pf*RON2, *Pf*RON4, *Pf*RON5, and *Pf*AMA1) was also identified in *Plasmodium falciparum* [7–9]. Attempts to knockout the AMA1 gene locus were unsuccessful in both *Plasmodium* [10] and *T. gondii* [11]. AMA1-binding peptide R1 not only prevents RON–AMA1 complex interaction, but also blocks *P. falciparum* merozoite invasion into erythrocytes [9].

Although the cumulative evidence above strongly suggests that the conserved RON–AMA1 complex plays an essential role in merozoite invasion, it is yet to be clarified whether molecules other than RON2, RON 4, and RON 5, play roles in the formation of the moving junction complex and in the invasion process. The report on *T. gondii* rhoptry proteome identified the presence of other RON proteins, RON1 and RON3 [12]. Therefore, we were interested in

* Corresponding author. Cell-Free Science and Technology Research Center, Ehime University, Matsuyama, Ehime 790-8577, Japan. Tel.: +81 89 927 8277; fax: +81 89 927 9941.
E-mail address: tsuboi@ccr.ehime-u.ac.jp (T. Tsuboi).

1383-5769/$ – see front matter © 2011 Elsevier Ireland Ltd. All rights reserved.
doi:10.1016/j.parint.2011.01.001

identifying the ortholog of *tgron3* in *P. falciparum* and in characterizing its protein expression profile, subcellular localization, and role in the formation of the RON–AMA1 complex.

2. Materials and methods

2.1. Parasites

P. falciparum asexual stages (3D7 strain) were maintained in human erythrocytes (blood group O^+) *in vitro*, as previously described [13].

2.2. RNA isolation and cDNA synthesis

Total RNA was extracted from *P. falciparum* schizont-infected erythrocytes (purified by differential centrifugation on a 70%/40% Percoll/sorbitol gradient) using the TRizol Reagent (Invitrogen, Carlsbad, CA). Following DNase treatment, cDNA was generated with a random hexamer using the SuperScriptIII® First Strand Synthesis System (Invitrogen).

2.3. Antibodies

Recombinant *Pf*RON3 proteins were produced using the wheat germ cell-free translation system (CellFree Sciences, Matsuyama, Japan) as described previously [14–16]. Briefly, regions of the *Pf*RON3 gene encoding the deduced amino acid sequence, 927–1056 (*Pf*RON3_1) and 1686–1884 (*Pf*RON3_2), were PCR-amplified from *P. falciparum* 3D7 blood-stage cDNA and ligated into pEU-E01-GST-(TEV)-N2 (CellFree Sciences), an expression plasmid with an N-terminal glutathione S transferase (GST)-tag followed by a tobacco etch virus (TEV) protease cleavage site, designed specifically for the wheat germ cell-free protein expression. Oligonucleotide primers used in the PCR amplification were *Pf*RON3_XhoIF1 (5′-ctcgagGATATTCCATTAAAAGAAACCTATAAATT-3′) and *Pf*RON3_BamHIR1 (5′-ggatccCTAATGTGGGAACATTTCATGATTTGGTA-3′) for *Pf*RON3_1, and *Pf*RON3_XhoIF2 (5′-ctcgagGATTTTAAAGATAAATCAGATGATGATC-3′) and *Pf*RON3_BamHIR2 (5′-ggatccCTATTTTTTAGGTACATATATATTATATGGTC-3′) for *Pf*RON3_2 (XhoI and BamHI restriction sites are underlined). Both GST-*Pf*RON3_1 and GST-*Pf*RON3_2 were captured using a glutathione-Sepharose 4B column (GE Healthcare, Camarillo, CA), and eluted by on-column cleavage with 60 U of AcTEV protease (Invitrogen) after extensive washing with PBS. To generate anti-*Pf*RON3_1 and anti-*Pf*RON3_2 sera, female BALB/c mice were immunized subcutaneously with 20μg of purified *Pf*RON3_1 or *Pf*RON3_2 emulsified with Freund's adjuvant. A Japanese white rabbit was also immunized subcutaneously with 250μg of purified *Pf*RON3_1 or *Pf*RON3_2 emulsified with Freund's adjuvant. All immunizations were performed 3 times at 3-week intervals, and then antisera were collected 2 weeks after the third immunization. In a similar manner, mouse anti-*Pf*RAP1 (aa 1–782) antibody, mouse anti-*Pf*EXP2 (aa 25–287) antibody, mouse and rabbit anti-*Pf*AMA1 (aa 25–546) antibodies, and rabbit anti-GST antibody, were generated as control. Rabbit antisera against the *Pf*RON3_1 and *Pf*RON3_2 proteins were affinity purified using a column conjugated with recombinant *Pf*RON3_1 or *Pf*RON3_2 as ligands, respectively. Briefly, recombinant *Pf*RON3_1 or *Pf*RON3_2 was covalently linked to a HiTrap™ NHS-activated HP column (GE Healthcare) as manufacturer's recommendation. Rabbit antiserum was then applied to either the *Pf*RON3_1- or the *Pf*RON3_2-conjugated column. After an extensive washing step with 20 mM phosphate buffer (pH 7.0), antigen-specific IgGs were eluted with 0.1 M glycine–HCl (pH 2.5), and then immediately neutralized with 1 M Tris (pH 9.0). Mouse monoclonal anti-*Pf*RON4 antibody (26C64F12) [7] and anti-*Pf*RESA antibody (23/9) [17] were kind gifts from Jean F. Dubremetz (Université de Montpellier 2, France) and Robin F. Anders (La Trobe University, Australia), respectively.

2.4. SDS-PAGE and western blot analysis

P. falciparum cultured parasites were harvested after tetanolysin (List Biological Laboratories, Inc., Campbell, CA) treatment that can remove the hemoglobin without loss of parasite proteins present in the parasitophorous vacuolar space [18]. The parasite proteins were then extracted in SDS-PAGE loading buffer, incubated at 4 °C for 6 h, and subjected to electrophoresis under reducing condition on a 12.5% polyacrylamide gel (ATTO, Tokyo, Japan). Proteins were then transferred to a 0.2-μm PVDF membrane (GE Healthcare). The proteins were immunostained with antisera followed by horseradish peroxidase-conjugated secondary antibody (GE Healthcare) and visualized with Immobilon Western Chemiluminescent HRP Substrate (Millipore, Billerica, MA) on a LAS 4000 mini luminescent image analyzer (GE Healthcare). The relative molecular masses of the proteins were estimated with reference to Precision Plus Protein Standards (BioRad, Hercules, CA).

2.5. Immunoprecipitation

Immunoprecipitation was carried out as previously described [19]. Briefly, proteins were extracted from late schizont parasite pellets in PBS with 1% Triton X-100 containing Complete Proteinase Inhibitor Cocktail (Roche, Indianapolis, IN). Supernatants (50 μl) were pre-incubated at 4 °C for 1 h with 40 μl of 50% protein G-conjugated beads (GammaBind Plus Sepharose; GE Healthcare) in NETT buffer (50 mM Tris–HCl, 0.15 M NaCl, 1 mM EDTA, and 0.5% Triton X-100) supplemented with 0.5% BSA (fraction V; Sigma-Aldrich Corporation, St. Louis, MO). Aliquots of recovered supernatants were incubated either with rabbit anti-*Pf*RON3_1, anti-*Pf*AMA1, anti-*Pf*RON2, or anti-GST antibody, and then 40 μl of 50% protein G-conjugated bead suspension was added. After one-hour incubation at 4 °C, the beads were washed once with NETT–0.5% BSA, once with NETT, once with high-salt NETT (0.5 M NaCl), once with NETT, and once with low-salt NETT (0.05 M NaCl and 0.17% Triton X-100). Finally, proteins were eluted from the protein G-conjugated beads with 0.1 M glycine–HCl (pH 2.5), and then immediately neutralized with 1 M Tris pH 9.0. The supernatants were used for western blot analysis.

2.6. Indirect immunofluorescence assay

Thin smears of ring or schizont-enriched *P. falciparum*-infected erythrocytes were prepared on glass slides and stored at −80 °C. The smears were thawed, fixed with 4% formaldehyde at room temperature for 10 min, permeabilized with PBS containing 0.1% Triton X-100 at room temperature for 15 min, and blocked with PBS containing 5% non-fat milk at 37 °C for 30 min. The smears were then incubated with rabbit anti-*Pf*RON3 antibodies (1:500 dilution) and control mouse antibodies at 37 °C for 1 h, followed by incubation with both Alexa Fluor 488-conjugated goat anti-rabbit IgG and Alexa Fluor 546-conjugated goat anti-mouse IgG (Invitrogen) as secondary antibodies (1:500) at 37 °C for 30 min. Nuclei were stained with 4′,6-diamidino-2-phenylindole (2 μg/ml, DAPI) mixed with a secondary antibody solution. Slides were mounted in ProLong Gold Antifade reagent (Invitrogen) and viewed under ×63 oil-immersion lens. High-resolution image-capture and processing were performed using a confocal scanning laser microscope (LSM5 PASCAL or LSM710; Carl Zeiss MicroImaging, Thornwood, NY). Images were processed in Adobe Photoshop (Adobe Systems Inc., San José, CA).

2.7. Immunoelectron microscopy

Parasites were fixed for 15 min on ice in a mixture of 1% paraformaldehyde and 0.1% glutaraldehyde in 0.1 M phosphate buffer (pH 7.4). Fixed specimens were washed, dehydrated, and embedded in LR White resin (Polysciences, Inc., Warrington, PA) as previously

have been described [20,21]. Ultrathin sections were blocked in PBS containing 5% non-fat milk and 0.01% Tween 20 (PBS-MT) at 37 °C for 30 min. Grids were then incubated at 4 °C overnight with rabbit anti-*Pf*RON3_2 or control sera in PBS-MT (1:20). After washing with PBS containing 10% BlockAce (Yukijirushi, Sapporo, Japan) and 0.01% Tween 20 (PBS-BT), the grids were incubated at 37 °C for 1 h with goat anti-rabbit IgG conjugated to 10 nm gold particles (GE Healthcare) diluted 1:20 in PBS-MT, rinsed with PBS-BT, and fixed at room temperature for 10 min in 2.5% glutaraldehyde to stabilize the gold particles. The grids were then rinsed with distilled water, dried, and stained with uranyl acetate and lead citrate. Samples were examined with a transmission electron microscope (JEM-1230; JEOL, Tokyo, Japan).

3. Results

3.1. Primary structure analysis of the RON3 orthologs

Using *Tg*RON3 (TGME49_023920) as a query in BLAST analyses [22], we found RON3 orthologs in *P. falciparum* (*Pf*RON3; PFL2505c, PlasmoDB) [23], *P. yoelii* 17XNL strain (*Py*RON3; PY01808, PlasmoDB), *P. vivax* Sal-I strain (*Pv*RON3; PVX_101485, PlasmoDB), *P. knowlesi* H strain (*Pk*RON3; PKH_146960, PlasmoDB), *P. chabaudi* AS strain (*Pch*RON3; PCA_146710, PlasmoDB), *P. berghei* ANKA strain (*Pb*RON3; PBANKA_146490, PlasmoDB), and *Eimeria tenella* (*Et*RON3; CAO79912, Sanger Institute). The full-length *Pf*RON3 protein consists of 2215 amino acid residues, with a putative N-terminal signal peptide sequence predicted by SignalP3.0 [24] to span amino acid residues 1–22. Three transmembrane regions (TM) (aa 250–272, 276–298, and 551–573) were predicted by TMHMM2.0 [25], and one coiled coil region (aa 1822–1847) was predicted by SMART [26]. Alignment of the deduced amino acid sequences of all the RON3 orthologs among the genus *Plasmodium* using Clustal W [27] demonstrated that twelve Cys residues are conserved (Fig. 1), with a 42% overall sequence identity. Moreover, the N-terminal region is highly conserved among the RON3 orthologs in the genus *Plasmodium*, in *T. gondii*, and in *E. tenella* (Fig. 2).

3.2. PfRON3 is expressed in the schizont stage and existed in the ring stage

The PfRON3 protein expression profile was analyzed by stage-specific western blot analysis using tightly synchronized parasites as antigens. Both antibodies (α-*Pf*RON3_1 and _2) recognized a band slightly larger than 250 kDa corresponding to the predicted molecular mass of *Pf*RON3 in late stage parasites, 40–44 h post invasion (Fig. 3A, arrowhead). Furthermore, both antibodies also recognized a prominent 190-kDa band, 40–44 h post invasion (Fig. 3A, arrow). After erythrocyte invasion, the 190-kDa band quickly degraded to 50- and 40-kDa bands (Figs. 3A and 4H). However, a small amount of the 190-kDa band was present throughout the ring (Figs. 3A and 4H) and trophozoite stages (Fig. 3A, 24–36 h). Additionally, only the anti-*Pf*RON3_2 antibody recognized a 37-kDa band, 40–44 h post invasion that might represent one of the processed forms of the *Pf*RON3 protein (Fig. 3A). Neither anti-PfRON3_1 or -PfRON3_2 had any reactivity against antigens of uninfected erythrocytes (Supplementary Fig. S1).

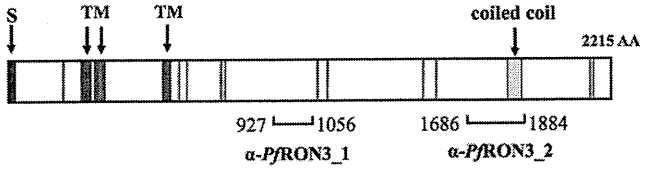

Fig. 1. Schematic representation of *Pf*RON3. The primary structure of *Pf*RON3 is depicted based on the analyses described in the Results section. S and TM indicate putative signal peptide (black) and transmembrane (blue) sequences, respectively. The yellow color box indicates a coiled coil region. Vertical red bars indicate conserved Cys residues in orthologs among the genus *Plasmodium*. The regions used to generate anti-*Pf*RON3 sera (α-*Pf*RON3_1 and α-*Pf*RON3_2) are indicated.

3.3. PfRON3 localizes in the rhoptry body of merozoites

In order to determine the sub cellular localization of *Pf*RON3, a dual label indirect immunofluorescence assay (IFA) was performed using anti-*Pf*RON3_2 antibody with anti-*Pf*RAP1 (rhoptry body marker), anti-*Pf*RON2 (rhoptry neck marker), anti-*Pf*AMA1 (microneme marker), and anti-*Pf*RESA (dense granule marker) antibodies as controls (Fig. 4). In mature schizonts, the anti-*Pf*RON3 antibody produced a punctate pattern of fluorescence in the apical end of each developing merozoite. Although some of the *Pf*RON3 signals overlapped with those of *Pf*RON2, *Pf*AMA1, or *Pf*RESA the *Pf*RON3 signals did not completely colocalize with those of the controls, whereas complete colocalization was observed between the signals of PfRON3 and *Pf*RAP1. Negative control sera were always used and these images were found to be negative (data not shown). To confirm the IFA results, the precise subcellular localization of *Pf*RON3 in the merozoite. Using anti-*Pf*RON3 antibody, gold particle signals were detected in the body portion of the rhoptries (Fig. 5).

3.4. PfRON3 is found in the parasitophorous vacuolar space after merozoite invasion into erythrocyte

To investigate *Pf*RON3 localization after the parasite invades erythrocytes, we performed IFA on ring stage parasites. *Pf*RAP1 and *Pf*EXP2 were used as parasitophorous vacuolar (PV) markers because they have been demonstrated to be present in ring stages and to associate with the PV [28–30]. We found that *Pf*RON3 colocalized with the PV markers, *Pf*RAP1 and *Pf*EXP2 in a discrete compartment surrounding the ring stage parasites (Fig. 6A). Next we performed western blot analysis using extracts of tightly synchronized ring or schizont stage parasites (Fig. 6B). *Pf*RON3 was detected in ring and schizont stage parasites together with *Pf*RAP1 and *Pf*EXP2. However *Pf*RON2 and *Pf*RON4 were detected only in schizont stage parasites (Fig. 6B) in agreement with the IFA results (Fig. 6A). Negative control sera were always used and these images were found to be negative (data not shown).

3.5. PfRON3 forms a complex with PfRON2 and PfRON4, but not with PfAMA1

To evaluate the interaction between *Pf*RON3 and the RON–AMA1 complex, we performed immunoprecipitation experiments using mature schizont-rich parasite extracts (Fig. 7). We did not detect *Pf*RON3 in the immunoprecipitate obtained using anti-*Pf*AMA1 antibody. However, PfRON3 was found in the anti-*Pf*RON2 precipitates. In the reciprocal experiment, *Pf*RON2 and *Pf*RON4 were detected in the immunoprecipitate obtained using the anti-*Pf*RON3_1 antibody; however, *Pf*AMA1 was not detected (Fig. 7). There was negligible crossreactivity between the anti-PfRON3_1 or anti-PfRON3_2 IgGs and PfRON2 and PfRON4 (Supplementary Fig. S1). These faint crossreactions were insignificant compared to the reactions with the actual target molecules.

4. Discussion

In this study, we characterized the protein expression profile and subcellular localization of *P. falciparum* RON3 as well as its complex formation with *Pf*RON2 and *Pf*RON4.

Studies of the apicomplexan parasite *T. gondii* identified various *Tg*RON proteins (RON2, RON4, RON5 [5,6], RON1, and RON3 [12]). The potential orthologs of the *Tg*RON proteins were subsequently

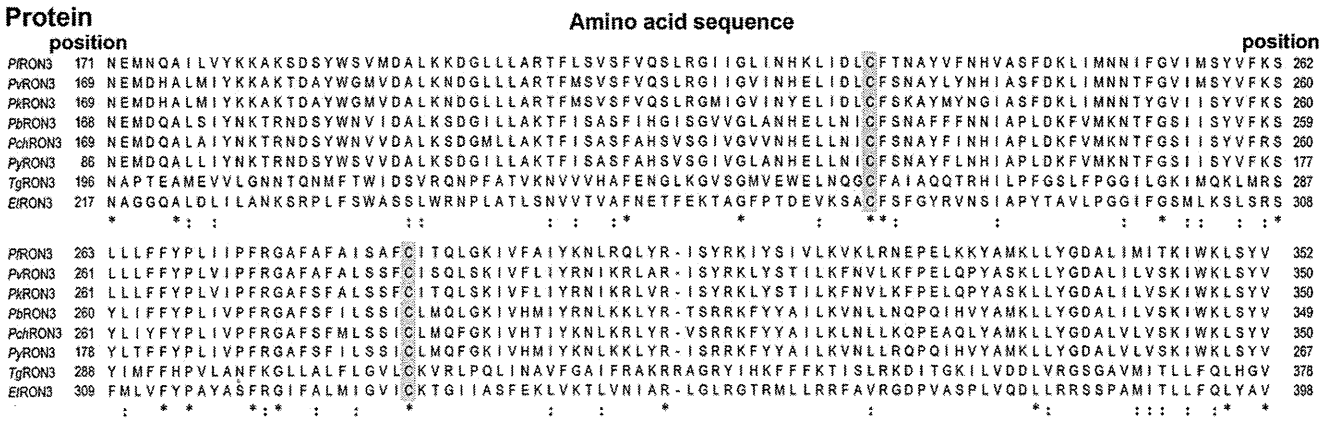

Fig. 2. Amino acid alignment of the conserved N-terminal region of RON3 orthologs. Deduced amino acid sequences of RON3 orthologs were aligned using Clustal W with manual correction. "*" indicates the conserved residues in the aligned sequences. ":" indicates conservative substitutions. Cys residues are highlighted in yellow.

identified in *P. falciparum*. Bradley et al. [12] suggested that *Pf*RON3 (PFL2505c) is an ortholog of *Tg*RON3 (TGME49_023920). However, Proellocks et al. [31] analyzed the amino acid sequence similarities of the RON orthologs identified in the genera *Plasmodium, Toxoplasma,* and some (but not all) *Apicomplexa*, and reported that, they may not be true orthologs because the collective sequence identity is below 12% [31]. In contrast, our pair-wise amino acid alignments between *T. gondii* and *P. falciparum* RON orthologs showed 11% identity between RON1 orthologs (TGME49_110010 vs. PFD0207c), 14% between RON2 orthologs(TGME49_100100 vs. PF14_0495), 12% between RON3 orthologs (TGME49_023920 vs. PFL2505c), and 10% between RON4 orthologs (TGME49_029010 vs. PF11_0168), suggesting that the amino acid identity between RON3 orthologs (*Tg*RON3 and *Pf*RON3) is comparable to that of other RON orthologs. Furthermore, multiple alignments of the deduced amino acid sequences of apicomplexan parasite RON3 orthologs showed that the N-terminal regions are conserved (Fig. 2). Based on these analyses, we conclude that *Pf*RON3 (PFL2505c) is an authentic ortholog of *Tg*RON3 (TGME49_023920).

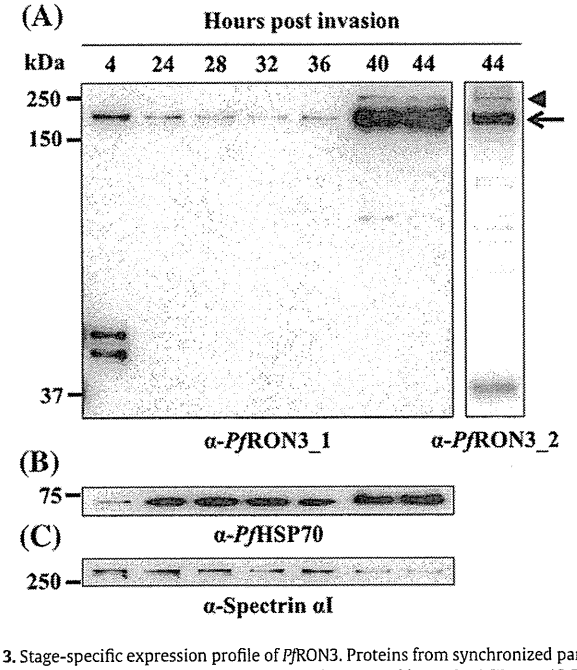

Fig. 3. Stage-specific expression profile of *Pf*RON3. Proteins from synchronized parasite cultures were harvested at each time point and separated by SDS-PAGE on a 12.5% gel under reducing condition. (A) Using either anti-*Pf*RON3_1- or anti-*Pf*RON3_2- specific antibodies, a band of approximately 260 kDa (arrowhead) was detected in late stages (40–44 h post invasion) and a 190-kDa band (arrow) was detected in both the schizont, ring, and trophozoite stage parasites. (B and C) Loading controls. To ensure that equal amounts of the stage-specific samples were loaded in each lane for western blot analysis, the membranes were probed with anti-*Pf*HSP70 monoclonal antibody (4C9) as a quantitative parasite protein marker [36], and anti-human spectrin α I rabbit antibody indicating the number of erythrocytes. The intensity of the *Pf*HSP70 bands indicated that the amount of sample loaded in each lane was comparable.

T. gondii RON3 protein was originally suggested to be localized at the rhoptry neck by immunofluorescence assay [12]. In contrast, our current immunoelectron microscopy results confirmed that *Pf*RON3 localizes in the rhoptry body rather than the rhoptry neck. Since *Pf*RON3 is in the rhoptry body, we are tempted to think that TgRON3 is also localizes in the rhoptry body rather than the rhoptry neck. Therefore we believe that the localization of *Tg*RON3 should be reconfirmed by electron microscopy using quality antibodies. In general, the biggest technical hurdle to obtaining antibodies of adequate quality for use in electron microscopy studies of this sort would be the ability to produce correctly folded recombinant proteins in sufficient quantity and purity [31]. The immunoelectron microscopy results we obtained clearly demonstrate that high quality antibodies can be successfully produced using quality proteins synthesized in the wheat germ cell-free protein production system. We have already [14–16] demonstrated that the wheat germ cell-free protein production system enables the expression of quality recombinant proteins without codon optimization.

In our stage-specific western blot and immunofluorescence microscopy analyses for the *Pf*RON3 expression profile, we detected *Pf*RON3 not only in the merozoite rhoptry body but also in the PV of ring stage parasites (Fig. 6). Previous studies showed that well-characterized rhoptry body proteins (*Pf*RhopH complex, *Pf*RAP complex, and *Pf*RAMA) are discharged into the PV [32–34]. Therefore, the secretory pathway of *Pf*RON3 into the PV might be similar to that of these rhoptry body proteins. Additionally, since the 260-kDa band, corresponding to full-length *Pf*RON3, is only visible at the schizont stage (40–44 h post invasion) (Fig. 3A), the processed 190-kDa fragment may contain the functional domains throughout the parasite's asexual erythrocytic cycle.

Finally, our immunoprecipitation studies demonstrated that *Pf*RON2, *Pf*RON3, and *Pf*RON4, are able to interact and form a novel complex *in vitro*, even in the absence of *Pf*AMA1, indicating that the formation of this novel RON complex is independent of *Pf*AMA1. These results are in agreement with the previously published results showing that *Pf*RON2 and *Pf*RON4 are able to interact and form a complex independently, in the absence of *Pf*AMA1 and in the parasite; most AMA1 is not associated with complexes that contain *Pf*RON2 and *Pf*RON4 [35]. However, in this study we were unable to confirme the

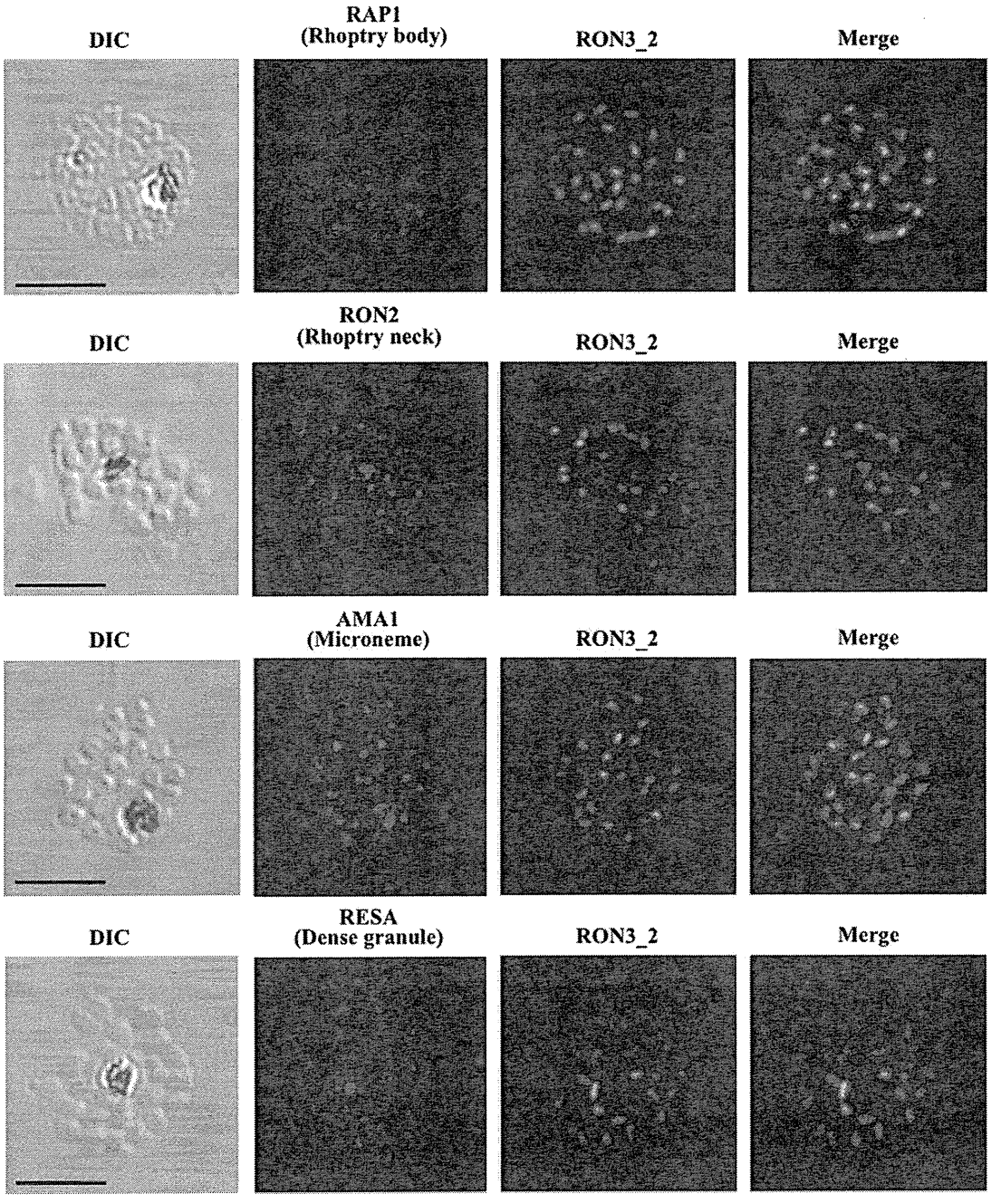

Fig. 4. *Pf*RON3 is expressed at the apical end of *Plasmodium* merozoites. Schizont and merozoite stage parasites were dual-labeled with antisera against *Pf*RON3_2 and either *Pf*RAP1 (rhoptry body marker), *Pf*RON2 (rhoptry neck marker), *Pf*AMA1 (microneme marker), or *Pf*RESA (dense granule marker). Nuclei are visualized with DAPI in merged images shown in the right panels. Bars represent 5 μm.

localization of *Pf*RON3 and the timing of the novel complex formation during the merozoite invasion process. Hence, the role of *Pf*RON3 and the novel complex in formation of the moving junction and the merozoite invasion process could not be elucidated. It will be interesting to undertake further experiments to shed light on the localization and function of *Pf*RON3 and the novel complex during merozoite invasion.

In summary, our results show that *Pf*RON3 is a rhoptry body protein, not a rhoptry neck protein, and that it interacts with *Pf*RON2 and *Pf*RON4, but not with *Pf*AMA1. These results suggest that *Pf*RON3 partakes in the novel *Pf*RON complex formation (*Pf*RON2, 3, and 4), but not in formation of the moving junction complex (*Pf*RON2, 4, 5, and *Pf*AMA1). The novel *Pf*RON complex, as well as the moving junction complex, might play a fundamental role in erythrocyte invasion by merozoite stage parasites.

Acknowledgments

We are grateful to Jean F. Dubremetz for providing the anti-*Pf*RON4 monoclonal antibody, Robin F. Anders for providing the anti-*Pf*RESA monoclonal antibody, and Niwat Kangwanrangsan for providing the mouse anti-*Pf*EXP2 antibody. We thank Masachika Shudo and Keizou Oka, Integrated Center for Science, Ehime University, Japan for technical assistance. We thank Thangavelu U. Arumugam for critical

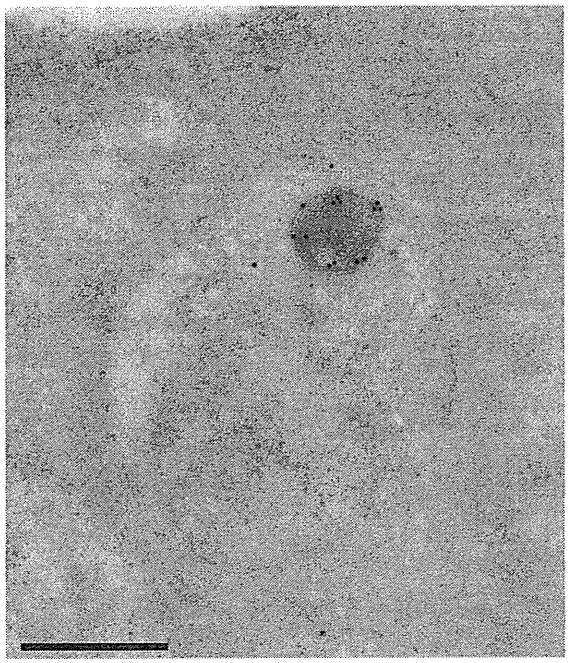

Fig. 5. Rhoptry body localization of *Pf*RON3 by immunoelectron microscopy. Longitudinally sectioned merozoites in mature schizonts were labeled with rabbit anti-*Pf*RON3_2 antibodies followed by secondary antibody conjugated with gold particles. The image shows that the gold particle signals were restricted to the merozoite rhoptry body. Bar represents 500 nm.

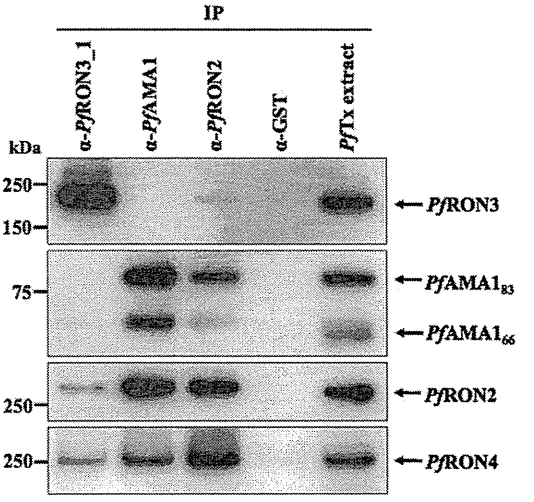

Fig. 7. *Pf*RON3 is not involved in the RON–AMA1 complex. Triton X-100 extracts of schizont-rich parasite (*Pf*Tx extract) were immunoprecipitated (IP) with rabbit sera against *Pf*RON3 (α-*Pf*RON3_1), *Pf*AMA1 (α-*Pf*AMA1), *Pf*RON2 (α-*Pf*RON2), or GST (α-GST), then stained with mouse antisera against *Pf*RON3, *Pf*AMA1, *Pf*RON2, or *Pf*RON4, respectively. Immunoprecipitation using anti-GST antibody was used as a negative control. No bands were detected in the anti-GST immunoprecipitate, indicating the exclusion of potential carryover of proteins due to insufficient or inadequate washing steps.

reading of the manuscript. This research was supported by the Ministry of Education, Culture, Sports, Science and Technology (21249028 and 21022034), and by the Ministry of Health, Labour,

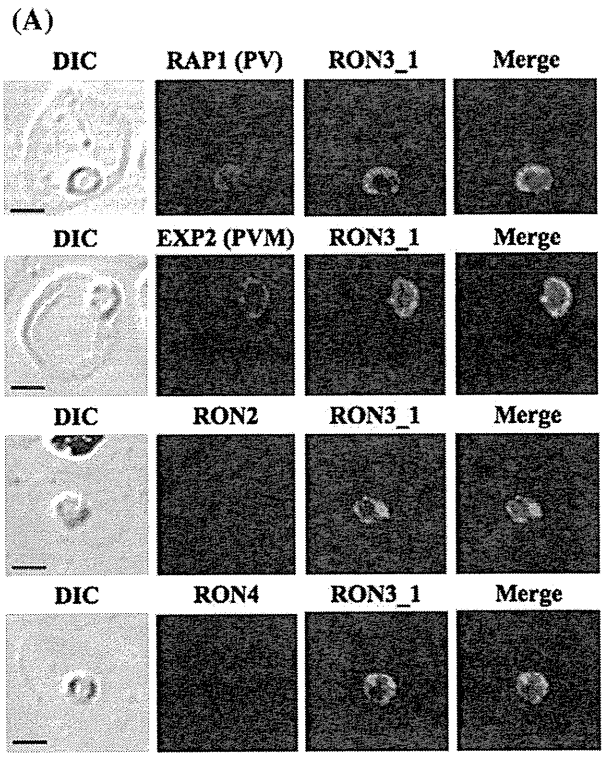

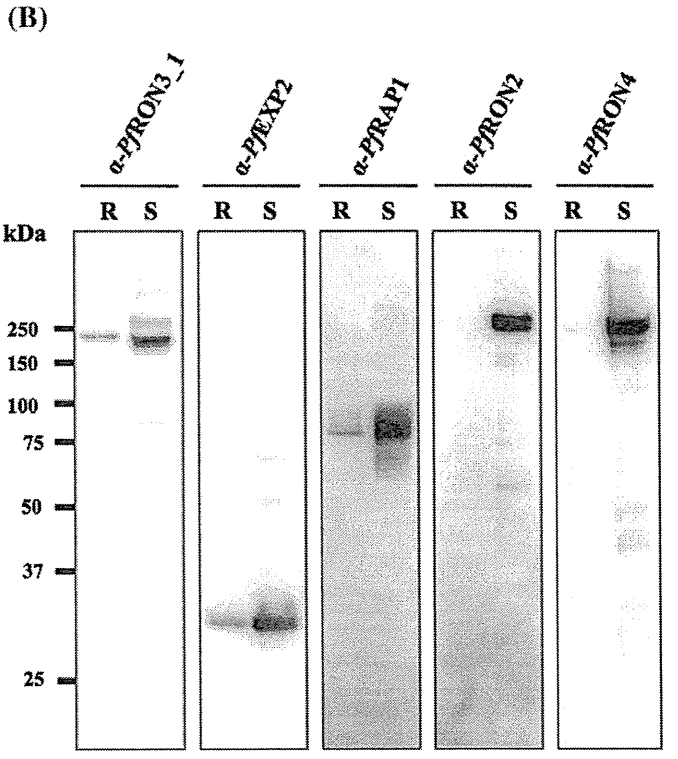

Fig. 6. *Pf*RON3 is found in the parasitophorous vacuole in ring stage parasites. (A) Ring stage parasites were dual-labeled with antisera against *Pf*RON3_1 and either *Pf*RAP1 (PV marker), *Pf*EXP2 (PVM marker), *Pf*RON2, or *Pf*RON4. Nuclei are visualized with DAPI in merged images shown in the right panels. Bars represent 2.5 μm. (B) Proteins from synchronized parasite cultures were harvested at the ring stage (R) and schizont stage (S), and separated by SDS-PAGE on a 12.5% gel under a reducing condition. After transfer of proteins onto a PVDF membrane, the membrane was stained using rabbit anti-*Pf*RON3_1, mouse anti-*Pf*RAP1, anti-*Pf*EXP2, anti-*Pf*RON2, anti-*Pf*RON4 antibodies.

and Welfare, Japan (H20-Shinkou-ippan-013 and H21-Chikyukibo-ippan-005).

Appendix A. Supplementary data

Supplementary data to this article can be found online at doi:10.1016/j.parint.2011.01.001.

References

[1] Hay SI, Guerra CA, Gething PW, Patil AP, Tatem AJ, Noor AM, et al. A world malaria map: *Plasmodium falciparum* endemicity in 2007. PLoS Med 2009;6:e1000048.
[2] Cowman AF, Crabb BS. Invasion of red blood cells by malaria parasites. Cell 2006;124:755–66.
[3] Kaneko O. Erythrocyte invasion: vocabulary and grammar of the *Plasmodium* rhoptry. Parasitol Int 2007;56:255–62.
[4] Aikawa M, Miller LH, Johnson J, Rabbege J. Erythrocyte entry by malarial parasites. A moving junction between erythrocyte and parasite. J Cell Biol 1978;77:72–82.
[5] Lebrun M, Michelin A, El Hajj H, Poncet J, Bradley PJ, Vial H, et al. The rhoptry neck protein RON4 re-localizes at the moving junction during *Toxoplasma gondii* invasion. Cell Microbiol 2005;7:1823–33.
[6] Alexander DL, Mital J, Ward GE, Bradley P, Boothroyd JC. Identification of the moving junction complex of *Toxoplasma gondii*: a collaboration between distinct secretory organelles. PLoS Pathog 2005;1:e17.
[7] Alexander DL, Arastu-Kapur S, Dubremetz JF, Boothroyd JC. *Plasmodium falciparum* AMA1 binds a rhoptry neck protein homologous to *Tg*RON4, a component of the moving junction in *Toxoplasma gondii*. Eukaryot Cell 2006;5:1169–73.
[8] Cao J, Kaneko O, Thongkukiatkul A, Tachibana M, Otsuki H, Gao Q, et al. Rhoptry neck protein RON2 forms a complex with microneme protein AMA1 in *Plasmodium falciparum* merozoites. Parasitol Int 2009;58:29–35.
[9] Richard D, MacRaild CA, Riglar DT, Chan JA, Foley M, Baum J, et al. Interaction between *Plasmodium falciparum* apical membrane antigen 1 and the rhoptry neck protein complex defines a key step in the erythrocyte invasion process of malaria parasites. J Biol Chem 2010;285:14815–22.
[10] Triglia T, Healer J, Caruana SR, Hodder AN, Anders RF, Crabb BS, et al. Apical membrane antigen 1 plays a central role in erythrocyte invasion by *Plasmodium* species. Mol Microbiol 2000;38:706–18.
[11] Hehl AB, Lekutis C, Grigg ME, Bradley PJ, Dubremetz JF, Ortega-Barria E, et al. *Toxoplasma gondii* homologue of *Plasmodium* apical membrane antigen 1 is involved in invasion of host cells. Infect Immun 2000;68:7078–86.
[12] Bradley PJ, Ward C, Cheng SJ, Alexander DL, Coller S, Coombs GH, et al. Proteomic analysis of rhoptry organelles reveals many novel constituents for host–parasite interactions in *Toxoplasma gondii*. J Biol Chem 2005;280:34245–58.
[13] Trager W, Jensen JB. Human malaria parasites in continuous culture. Science 1976;193:673–5.
[14] Tsuboi T, Takeo S, Iriko H, Jin L, Tsuchimochi M, Matsuda S, et al. Wheat germ cell-free system-based production of malaria proteins for discovery of novel vaccine candidates. Infect Immun 2008;76:1702–8.
[15] Tsuboi T, Takeo S, Sawasaki T, Torii M, Endo Y. An efficient approach to the production of vaccines against the malaria parasite. Meth Mol Biol 2010;607: 73–83.
[16] Tsuboi T, Takeo S, Arumugam TU, Otsuki H, Torii M. The wheat germ cell-free protein synthesis system: a key tool for novel malaria vaccine candidate discovery. Acta Trop 2010;114:171–6.
[17] Culvenor JG, Day KP, Anders RF. *Plasmodium falciparum* ring-infected erythrocyte surface antigen is released from merozoite dense granules after erythrocyte invasion. Infect Immun 1991;59:1183–7.
[18] Hiller NL, Akompong T, Morrow JS, Holder AA, Haldar K. Identification of a stomatin orthologue in vacuoles induced in human erythrocytes by malaria parasites. A role for microbial raft proteins in apicomplexan vacuole biogenesis. J Biol Chem 2003;278:48413–21.
[19] Kaneko O, Fidock DA, Schwartz OM, Miller LH. Disruption of the C-terminal region of EBA-175 in the Dd2/Nm clone of *Plasmodium falciparum* does not affect erythrocyte invasion. Mol Biochem Parasitol 2000;110:135–46.
[20] Torii M, Adams JH, Miller LH, Aikawa M. Release of merozoite dense granules during erythrocyte invasion by *Plasmodium knowlesi*. Infect Immun 1989;57: 3230–3.
[21] Aikawa M, Atkinson CT. Immunoelectron microscopy of parasites. Adv Parasitol 1990;29:151–214.
[22] Altschul SF, Madden TL, Schaffer AA, Zhang J, Zhang Z, Miller W, et al. Gapped BLAST and PSI-BLAST: a new generation of protein database search programs. Nucleic Acids Res 1997;25:3389–402.
[23] Bahl A, Brunk B, Crabtree J, Fraunholz MJ, Gajria B, Grant GR, et al. PlasmoDB: the *Plasmodium* genome resource. A database integrating experimental and computational data. Nucleic Acids Res 2003;31:212–5.
[24] Bendtsen JD, Nielsen H, von Heijne G, Brunak S. Improved prediction of signal peptides: SignalP 3.0. J Mol Biol 2004;340:783–95.
[25] Krogh A, Larsson B, von Heijne G, Sonnhammer EL. Predicting transmembrane protein topology with a hidden Markov model: application to complete genomes. J Mol Biol 2001;305:567–80.
[26] Schultz J, Milpetz F, Bork P, Ponting CP. SMART, a simple modular architecture research tool: identification of signaling domains. Proc Natl Acad Sci USA 1998;95: 5857–64.
[27] Thompson JD, Higgins DG, Gibson TJ. CLUSTAL W: improving the sensitivity of progressive multiple sequence alignment through sequence weighting, position-specific gap penalties and weight matrix choice. Nucleic Acids Res 1994;22:4673–80.
[28] Baldi DL, Andrews KT, Waller RF, Roos DS, Howard RF, Crabb BS, et al. RAP1 controls rhoptry targeting of RAP2 in the malaria parasite *Plasmodium falciparum*. EMBO J 2000;19:2435–43.
[29] Johnson D, Gunther K, Ansorge I, Benting J, Kent A, Bannister L, et al. Characterization of membrane proteins exported from *Plasmodium falciparum* into the host erythrocyte. Parasitology 1994;109(Pt 1):1–9.
[30] Fischer K, Marti T, Rick B, Johnson D, Benting J, Baumeister S, et al. Characterization and cloning of the gene encoding the vacuolar membrane protein EXP-2 from *Plasmodium falciparum*. Mol Biochem Parasitol 1998;92:47–57.
[31] Proellocks NI, Coppel RL, Waller KL. Dissecting the apicomplexan rhoptry neck proteins. Trends Parasitol 2010;26:297–304.
[32] Sam-Yellowe TY, Shio H, Perkins ME. Secretion of *Plasmodium falciparum* rhoptry protein into the plasma membrane of host erythrocytes. J Cell Biol 1988;106: 1507–13.
[33] Howard RF, Stanley HA, Campbell GH, Reese RT. Proteins responsible for a punctate fluorescence pattern in *Plasmodium falciparum* merozoites. Am J Trop Med Hyg 1984;33:1055–9.
[34] Topolska AE, Lidgett A, Truman D, Fujioka H, Coppel RL. Characterization of a membrane-associated rhoptry protein of *Plasmodium falciparum*. J Biol Chem 2004;279:4648–56.
[35] Collins CR, Withers-Martinez C, Hackett F, Blackman MJ. An inhibitory antibody blocks interactions between components of the malarial invasion machinery. PLoS Pathog 2009;5:e1000273.
[36] Tsuji M, Mattei D, Nussenzweig RS, Eichinger D, Zavala F. Demonstration of heat-shock protein 70 in the sporozoite stage of malaria parasites. Parasitol Res 1994;80:16–21.

Acta Tropica 113 (2010) 61–65

Contents lists available at ScienceDirect

Acta Tropica

journal homepage: www.elsevier.com/locate/actatropica

Detection of *Plasmodium vivax* infection in the Republic of Korea by loop-mediated isothermal amplification (LAMP)

Jun-Hu Chen[a,b], Feng Lu[a,c], Chae Seung Lim[d], Jung-Yeon Kim[e], Heui-June Ahn[f], In-Bum Suh[g], Satoru Takeo[h], Takafumi Tsuboi[h], Jetsumon Sattabongkot[i], Eun-Taek Han[a,*]

[a] Department of Parasitology, Kangwon National University College of Medicine, Hyoja2-dong, Chunchon, Gangwon-do 200-701, Republic of Korea
[b] Institute of Parasitic Diseases, Zhejiang Academy of Medical Sciences, Hangzhou 310013, People's Republic of China
[c] Jiangsu Institute of Parasitic Diseases, Wuxi 214064, People's Republic of China
[d] Department of Laboratory Medicine, College of Medicine, Korea University, Seoul 425-707, Republic of Korea
[e] Department of Malaria and Parasitic Disease, National Institute of Health, KCDC, Seoul 122-701, Republic of Korea
[f] Department of Internal Medicine, Korea Institute of Radiological and Medical Sciences, Seoul 139-706, Republic of Korea
[g] Department of Laboratory Medicine, Kangwon National University College of Medicine, Chunchon 200-701, Republic of Korea
[h] Cell-free Science and Technology Research Center and Venture Business Laboratory, Ehime University, Matsuyama 790-8577, Japan
[i] Department of Entomology, Armed Forces Research Institute of Medical Sciences, Bangkok 10400, Thailand

ARTICLE INFO

Article history:
Received 31 October 2008
Received in revised form
10 September 2009
Accepted 14 September 2009
Available online 22 September 2009

Keywords:
Malaria
Plasmodium vivax
LAMP
Diagnosis
Republic of Korea

ABSTRACT

Loop-mediated isothermal amplification (LAMP) is a novel technique that rapidly amplifies target DNA in isothermal conditions. In a previous study, the sensitivities and specificities of LAMP, microscopy, and nested PCR were compared in the context of rapid malaria detection. In the present study, LAMP detected vivax malaria parasites in 115 of 117 microscopically positive samples (sensitivity, 98.3%; 95% CI, 97.4–100%), which agreed well with the nested PCR results (sensitivity, 99.1%; 95% CI: 96.0–100%). No positive cases of malaria were detected by LAMP or nested PCR in 50 consecutive feverish patients other than malaria from malaria endemic areas. LAMP performed on DNA extracted from heat-treated blood had a sensitivity of 93.3% (28/30, 95% CI: 84.4–100%) and specificity of 100% (30/30, 95% CI: 100%). The present study shows that LAMP based assays have high sensitivity, specificity, and amplification efficiencies for *Plasmodium vivax* detection. The authors recommend that LAMP can be considered as a rapid nucleic acid amplification assay for the molecular diagnosis of *P. vivax* in both clinical laboratories and malaria clinics in areas where vivax malaria is endemic.

1. Introduction

Forty percent of the world's population is threatened by *Plasmodium vivax* and there are millions of clinical infections annually. Although *P. vivax* infections are often regarded as benign and self-limited, recent evidence indicates that the overall burden, economic impact, and disease severity of *P. vivax* infections have been underestimated (Price et al., 2007). Malaria control and treatment strategies depend largely on laboratory-confirmed diagnoses and the present lack of an affordable, reliable diagnostic method is a major obstacle because of misdiagnoses and treatment delays.

Microscopic examinations of blood smears are still considered to be the best means of detecting malaria. Such examinations are cheap and straightforward, but are also labor-intensive, time-consuming, and require well-trained personnel (Mens et al., 2007). However, a variety of rapid diagnostic tests (RDTs) for malaria have been recently developed. These tests have rapid turnaround times (15–20 min), are easy of use, and require no electricity supply or dedicated equipment, which means that inexperienced laboratory and clinical staff can make diagnoses (Moody, 2002). However, these tests are based on the recognition of *Plasmodium* antigens in blood and the current RDTs for *P. vivax* lack sufficient sensitivity for the detection of vivax malaria (van den Broek et al., 2006). On the other hand, PCR (polymerase chain reaction) based methods, such as nested PCR, use species-specific primers for DNA amplification and are able to detect parasitemias as low as 1 parasite/μl (Snounou et al., 1993), but protracted turnaround times, high costs, and the availability of a well-equipped laboratory render this technology unsuitable for routine diagnosis in hospital laboratories and field clinics in endemic areas (Hanscheid and Grobusch, 2002).

Recently, a new, simple, sensitive technique, loop-mediated isothermal amplification (LAMP), was developed to detect the highly conserved 18S ribosomal RNA gene of *P. vivax* (Notomi et al., 2000; Han et al., 2007). LAMP involves autocycling strand displacement DNA synthesis by *Bacillus stearothermophilus* (*Bst*) DNA polymerase using a set of six primers to produce stem-loop DNA

* Corresponding author. Tel.: +82 33 250 7941; fax: +82 33 255 8809.
E-mail addresses: ethan@kangwon.ac.kr, etaekhan@yahoo.com (E.-T. Han).

0001-706X/$ – see front matter © 2009 Elsevier B.V. All rights reserved.
doi:10.1016/j.actatropica.2009.09.007